Micron 40 (2009) 669–690

Contents lists available at ScienceDirect

Micron

journal homepage: www.elsevier.com/locate/micron

Review

Studies on molluscan shells: Contributions from microscopic and analytical methods

Silvia Maria de Paula, Marina Silveira *

Instituto de Física, Universidade de São Paulo, 05508-090 São Paulo, SP, Brazil

ARTICLE INFO

Article history:
Received 25 April 2007
Received in revised form 7 May 2009
Accepted 10 May 2009

Keywords:
Mollusca
Shell microstructures
Electron microscopy
Infrared spectroscopy
X-ray diffraction
Electron diffraction

ABSTRACT

Molluscan shells have always attracted the interest of researchers, from biologists to physicists, from paleontologists to materials scientists. Much information is available at present, on the elaborate architecture of the shell, regarding the various Mollusc classes. The crystallographic characterization of the different shell layers, as well as their physical and chemical properties have been the subject of several investigations. In addition, many researches have addressed the characterization of the biological component of the shell and the role it plays in the hard exoskeleton assembly, that is, the biomineralization process. All these topics have seen great advances in the last two or three decades, expanding our knowledge on the shell properties, in terms of structure, functions and composition. This involved the use of a range of specialized and modern techniques, integrating microscopic methods with biochemistry, molecular biology procedures and spectroscopy. However, the factors governing synthesis of a specific crystalline carbonate phase in any particular layer of the shell and the interplay between organic and inorganic components during the biomineral assembly are still not widely known.

This present survey deals with microstructural aspects of molluscan shells, as disclosed through use of scanning electron microscopy and related analytical methods (microanalysis, X-ray diffraction, electron diffraction and infrared spectroscopy). These already published data provide relevant information on shells and also contribute for better understanding the biomineralization process.

Contents

* Corresponding author at: Lab. de Microscopia Eletrônica, Instituto de Física, Univ. de São Paulo, C.P. 66318, CEP 05314-970, São Paulo, SP, Brazil. Tel.: +55 11 3091 6854; fax: +55 11 3813 4334.
E-mail addresses: moranelli@gmail.com (S.M. de Paula), msilveir@if.usp.br (M. Silveira).

0968-4328/$ – see front matter © 2009 Elsevier Ltd. All rights reserved.
doi:10.1016/j.micron.2009.05.006

1. Introduction

Molluscan shells are typical biocomposites, essentially consisting of calcium carbonate crystals associated with an organic matrix resulting in a lightweight product of highly elaborate morphologies, endowed with unique structural properties. The organic matrix is synthesized in the extrapallial compartment of the animal and provides the framework upon which the inorganic crystals nucleate, become oriented and grow (Wilbur, 1972; Simkiss and Wilbur, 1989; Addadi et al., 2006; Nudelman et al., 2006). This crystallization process of shell calcium carbonate is a lifelong incremental activity that depends on several intrinsic and environmental factors.

It is well known that only two major phases of calcium carbonate, aragonite and calcite are present in the structure of shells, which are organized in three layers: the innermost layer is the aragonitic nacre and the outer one, usually prismatic, is comprised of either aragonite or calcite. In between, a layer of obliquely crossed crystals – the crossed-lamellar layer, is frequently present. The entire structure is externally covered with uncalcified periostracum. This is a generalized and oversimplified shell model, as there are many combinations of structural patterns, characteristic of the several classes, as detailed in Watabe (1984, 1988).

Molluscan shells act as a system of choice for biomineralization studies. Compared to other composite materials, shell presents superior mechanical properties (stiffness, fracture toughness, tensile strength) due to a complex architecture and the involvement of biological macromolecules (Weiner and Addadi, 1997; Currey, 1999; Checa et al., 2005). At present, many reports are available about the intricate organization of the mineral phases (Grégoire, 1972; Carter, 1980a; Wilbur and Saleuddin, 1983); the crystallographic orientation within individual layers (Chateigner et al., 2000; Feng et al., 2000a; DiMasi and Sarikaya, 2004); the influence of the biological phase on crystalline species (Grégoire, 1972; Pereira-Mouriès et al., 2002a) and on the properties of biological components (Weiner and Traub, 1980; Simkiss and Wilbur, 1989; Chateigner et al., 2000). Such knowledge is likely to help the synthesis of materials for technological and biomedical applications (Kaplan, 1998). As noted by several investigators (Mann, 1996; Lin and Meyers, 2000), understanding the principles and processes involved in mineralizing biological systems would considerably contribute to the development of new "biomimetic" materials. Many experimental approaches addressing these topics are underway (Meldrum, 2003).

Besides this current interest, fossil molluscan shells are valued markers in stratigraphic and paleoecological studies (Carter, 1990a). Fossilized calcified parts present additional criteria for phylogenetic studies on this group of animals (Salvini-Plawen, 1980). Structural and microstructural features of shells (Carter, 1980b; Hickman, 2004; Checa et al., 2005; Taylor and Reid, 1990) are valuable in ascertaining systematic and evolutionary relationships within the phylum Mollusca. Comprehensive reviews are available on all the above topics (Grégoire, 1972; Wilbur, 1972; Watabe, 1984, 1988).

More recently, important data relating structural details of the shell to a biological activity were obtained, as resultant from the application of modern techniques, some of which were formerly restricted to biologists. It is well known that formation of the mineral phase of the shell is closely associated with the biological matrix, essentially comprised of polysaccharide β-chitin and glycoproteins. The presence of chitin was demonstrated in several instances, by different means: Weiner and Traub (1980) used X-ray diffraction; Weiss et al. (2002a) applied chemical and biochemical reactions and nuclear magnetic resonance; Weiss and Schönitzer (2006) utilized confocal laser scanning microscopy to characterize chitin during the larval shell developmental stages. Weiss et al. (2002b) were also able to detect the presence of an amorphous calcium carbonate phase in early developmental stages of bivalve shells, using infrared and Raman image spectroscopy, polarization microscopy, as well as scanning electron microscopy (SEM).

The distribution of macromolecules within the organic matrix could be detected in nacre crystals of *Nautilus* by means of immunotechniques and SEM (Nudelman et al., 2006). X-ray diffraction and SEM were applied in texture analyses of shell layers by Checa (2000). High resolution images of the biological matrix were obtained in *Atrina serrata*, by cryo-transmission electron microscopy (Levi-Kalisman et al., 2001). Atomic force microscopy was used by Giles et al. (1995) in *in situ* experiments to locate sites of aragonite overgrowth in the same genus, *Atrina* sp. Several matrix proteins that are very important for the biomineralization processes were identified in the various shell layers by Zhang and Zhang (2006), using molecular genetic techniques. Similarly, proteins isolated from *Pinna nobilis* were characterized by SDS-PAGE techniques, molecular genetics and immunohistological methods (Marin and Luquet, 2004, 2005). A comprehensive view of the mineralizing role of these (very acidic) proteins in molluscs is provided in Marin and Luquet (2007). The biological matrix as a whole also was thoroughly characterized at the macromolecular level by Bezares et al. (2008). All these new achievements to mention just a selection, have considerably contributed to the understanding of mechanisms involved in shell biomineralization. In this particular process, known as biologically controlled (extracellular) mineralization, ions are nucleated outside the cell upon the matrix, i.e., the organic framework comprised of β-chitin and acidic macromolecules (Veis, 2003; Weiner and Dove, 2003). These biomineralization topics have been reviewed in several books (Simkiss and Wilbur, 1989; Mann, 1996; Dove et al., 2003), and in reviews and chapters (Carter, 1980a; Meldrum, 2003; Weiner and Dove, 2003). Carter (1980a,b, 1990a), provided a nearly complete guide for the identification of Bivalve shell structures. Gastropods shell organization was reviewed by Bandel (1990). In all these studies, electron microscopy has played a fundamental role, in the identification of minute structural details at a resolution well beyond that of light microscopy. An important landmark in the characterization of molluscan shells was established early in 1930 by O.B. Bøggild, who pioneered the application of polarization microscopy to sectioned specimens. However, this method is currently of limited use. According to Carter and Ambrose (1989), the merits of using polarization microscopy have been largely surpassed in favor of scanning electron microscopy. Historically, a great progress was also obtained with the use of X-ray diffraction techniques, followed by transmission electron microscopy. Modern methods of investigation also include other important tools, such as cryo-ultramicrotomy (Levi-Kalisman et al., 2001), atomic force microscopy (Giles et al., 1995; Weiner and Addadi, 1997; Sikes et al., 1998); high voltage TEM (Rousseau et al., 2005) and several analytical routes, such as electron

Table 1
Specimens used for morphological studies.

Taxon	Class/source
Anodontites trapezialis Lamarck, 1819	Bivalvia: freshwater. Itapecerica da Serra, SP
Macrocallista maculata Linnaeus, 1758	Bivalvia: Heterodonta, marine, uncertain origin
Achatina fulica Bowdich, 1822	Gastropoda: Stylommatophora, terrestrial, São Paulo
Pomacea lineata Spix, 1827	Gastropoda: freshwater, Heliário Modelo, São Paulo
Melanoides tuberculatus Müller, 1774	Gastropoda: freshwater, Ribeirão Pires, SP
Physa cubensis Pfeiffer, 1839	Gastropoda: freshwater, Ribeirão Pires, SP
Dentalium (s.l.)	Scaphopoda: marine (sand dweller) uncertain origin
Coccodentalium Sacco, 1896[(1)]	Scaphopoda: marine, 175 m deep mud, Atlantic coast[a]
Fustiaria Stoliczka, 1868[(1)]	Scaphopoda: marine, 175 m deep mud, Atlantic coast[a]
Plagyoglypta	Scaphopoda: marine, 175 m deep mud, Atlantic coast[a]
(+ two other unidentified shells)	Scaphopoda: marine, 175 m deep mud, Atlantic coast[a]

[a] Station 6606, W. Besnard ship 27°48.0′S; 47°24.1′W.

diffraction, microanalysis, chromatography, infrared (FTIR) and Raman spectroscopy (Addadi and Weiner, 1992; Checa, 2000; Fu et al., 2005). Preparative procedures especially devised for microstructural studies of shells are discussed in Carter and Ambrose (1989).

In 2 of this survey selected topics on shell microstructure and properties are reviewed. Data obtained from analytical methods are presented in 5. Original micrographs included throughout are from our specimens of Conchifera: Bivalvia, Gastropoda and Scaphopoda (Table 1). Shells of the bivalve and gastropods used herewith are well documented in Simone (2006). Spectroscopic essays were carried out with specimens listed in Table 2.

2. Morphological aspects

In addition to the protective exoskeleton, a remarkable number of mineralized structures occur in molluscs, like radula, operculum and darts. Simkiss and Wilbur (1989) recognized at least 26 of such structures, containing 20 mineral types. Other examples of aragonitic and calcitic structures in Gastropoda were provided by Bandel (1990). The shell itself is always composed of calcium carbonate crystals, arranged in a particular layering, characteristic for each of the six classes: Monoplacophora, Polyplacophora, Gastropoda, Bivalvia, Scaphopoda, and Cephalopoda. According to Carter (1990a), this crystals order constitutes the shell architecture, i.e., the orientation of the main crystalline layers, relative to the bulk of a shell. The basic arrangement of minor units is more significant than the architecture, such as rods, tablets and blades, in any given layer of the shell. These are the microstructures of a shell, clearly resolved through scanning electron microscopy, and that represent valuable criteria for shell identification. The following are major microstructural groups established by Carter (1980a) for bivalves:

Microstructural groups	Microstructural categories
1. Prismatic	1. Aragonitic prismatic
2. Spherulitic	2. Calcitic prismatic
3. Laminar	3. Nacreous, aragonitic
4. Crossed	4. Porcelaneous, aragonitic
5. Homogeneous	5. Foliated
6. Isolated spicules and spikes	6. Calcitic
7. Isolated crystal morphotypes	

Each of these groups and categories is divided into subgroups, all of them illustrated in Carter's Appendix 2B (Carter, 1980b). These data complement and extend those of Bøggild (1930) in his broad, light microscopic treatise on molluscan shells. In a subsequent publication, Carter (1990b) presented a glossary of terms and definitions pertaining to all mineralizing phyla, excluding protozoa. In most cases, microstructures observed in SEM coincide with the texture patterns characterized by X-ray, except for some more complex crystalline arrangements (Chateigner et al., 2000). A lack of uniformity is observed among different authors, regarding the identification and nomenclature of the various shell layers (see Watabe, 1984, 1988). Grégoire (1972) presented a concise classification of structures, based on data collected by scanning electron microscopy (SEM) and transmission electron microscopy (TEM), namely:

1. Homogeneous (HOM).
2. Prismatic.
3. Foliated.
4. Nacreous.
5. Grained.
6. Crossed-lamellar (CLL).
7. Complex crossed-lamellar (CCL).

In this review, Grégoire (1972) established a relation between the crystalline categories and their distribution in molluscs families or genera. A rather complete, and indeed valuable, table of data relates investigators, materials studied and abstracts of results regarding the organic components of shells, going back to 1900.

What follows is an attempt to review mollusc shell microstructure, as resultant from the application of microscopical methods; these data are, as far as possible, also correlated with available analytical investigations. In addition, incursions are made on the tubular shells of Scaphopoda. Comparatively, this smaller class of Molluscs has been given less attention, and will be considered separately.

2.1. Methodology

The routine preparation for scanning microscopy followed essentially that of Carter and Ambrose (1989): small shells or fractured parts of larger ones, un-polished and un-etched, were

Table 2
Calcium carbonate polymorphs observed in specific locations of molluscan shells.

Class	Species	Structure	Mineral	References
Gastropoda	*Haliotis laevigata*	Nacreous	Aragonite Amorphous $CaCO_3$	Nassif et al. (2005)
	Strombus gigas	Lamellar	Aragonite	Kamat et al. (2000)
Cephalopoda	*Nautilus pompilius*	Shell powder	Aragonite	Velázquez-Castillo et al. (2006)
Monoplacophora	*Micropilina arntzi*	Nacreous	Aragonite	Cruz et al. (2003)

sonicated in water, dried and coated with gold sputtering. Whole mounts of the insoluble organic matrix, isolated from shells of gastropods *Physa cubensis* and *Achatina fulica*, were studied in the light microscope, also using the conventional periodic acid-Schiff (PAS) cytochemical staining. For SEM studies, the matrices of both prismatic and nacreous layers of *Anodontites trapezialis* were obtained by decalcifying the shell in EDTA (6% solution followed by 8% solution, 1 week duration). After washing in water, they were impregnated with osmium tetroxide followed by tannin solutions, dehydrated in ethanol, critical point dried and gold sputtered. Except for Fig. 7C and D, SEM used throughout was a Jeol JSM 840-A, operated at 25 or 12 kV.

Fragments of periostracum of the same bivalve were fixed in glutaraldehyde/osmium tetroxide solutions, embedded in Epon resin, sectioned and stained for observation in a Philips CM-200 transmission electron microscope (TEM), operated at 160 kV. The hinge ligament of *A. trapezialis* was mechanically dissociated, sonicated in ethanol and spread onto carbon films for TEM studies; selected area electron diffractions (SAED) of these were obtained at 200 kV.

2.2. Microstructures

2.2.1. Prismatic structures

The outer crystalline layer of the molluscan shell, most prominent in bivalves, consists of either aragonitic or sometimes calcitic prisms. Carter (1980a) recognized four main categories of prismatic structures: simple prismatic, fibrous prismatic, spherulitic prismatic and composite prismatic. Grégoire (1972) reviewed earlier data on the mineral composition, crystallography and matrix–mineral relations of the prismatic layer, using X-ray diffraction, polarization microscopy and TEM. In bivalves, prisms align with their long axes perpendicular to the outer surface of the shell, i.e., they are vertically oriented under the periostracum, in a compact arrangement; however, in *Mytilus edulis*, a 45° inclination occurs (Feng et al., 2000a). This is clearly demonstrated using selected area electron diffraction and X-ray diffraction. In *Mytilus* and *Pinctada martensii*, investigated by Checa et al. (2005), in *Pinctada radiata* (Nakahara and Bevelander, 1971) and in other marine bivalves, the prisms are calcitic. As a rule, prisms are polycrystalline, created from longitudinally running units (Checa, 2000; Grégoire, 1967; Dauphin, 2003).

The scanning microscope shows "feather-like" surface structure in aragonitic prisms, due to variously oriented striations, whereas calcitic prisms show transverse periodicities, as if comprised of stacked disks (Grégoire, 1972; Checa, 2000). Fig. 1(A–D) illustrates well-formed, aragonitic, simple prismatic elements of *A. trapezialis*, also studied by Callil and Mansur (2005). The prisms reach about 1 mm high, have polygonal bases, mostly hexagonal, varying from 20 to 50 μm on side; the fractured surface is rough, demonstrating their polycrystalline character (Fig. 1B); see also Grégoire (1961, Fig. 7). Periodic growth lines are present on the prism faces of *A. trapezialis* (Fig. 1C, asterisks); a matrix cements the prisms together (Fig. 1C and D). A similar coat is

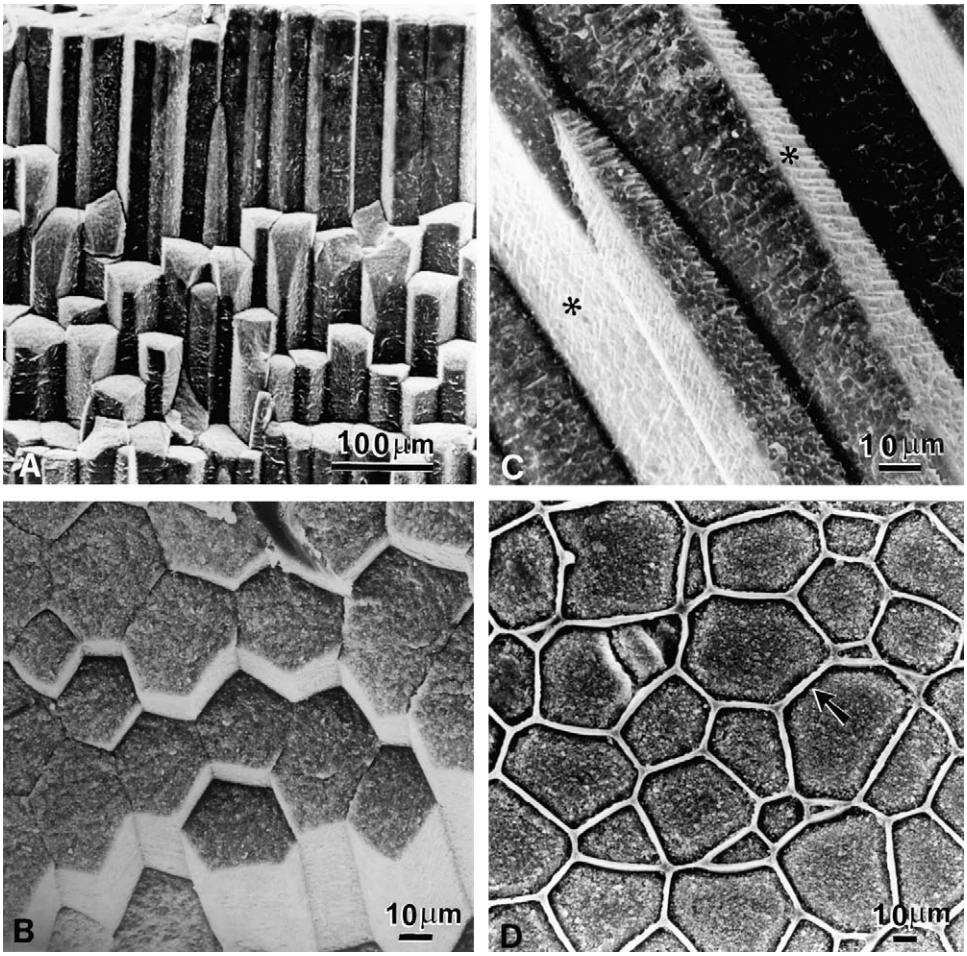

Fig. 1. Prismatic layer of *Anodontites trapezialis* shell (Bivalvia), fractured in a plane perpendicular to its outer surface. (A) The aragonitic simple prisms, about 1 mm high, were cut at different levels. (B) End-on view of the crystals showing hexagonal or pentagonal bases; their polycrystalline character is evident. (C) Periodic growth steps (*) and remains of the biological matrix decorate the lateral surfaces of all prisms. (D) Underside of the periostracum of another shell, showing continuity of the thick interprismatic matrix (arrowed). SEM, 25 kV.

present on the calcitic prisms of *P. nobilis* and *Pinctada margaritifera* (Dauphin, 2003). The prisms are embedded in a thick organic coat – the *conchiolin* layer of Grégoire (1961, 1972). Gastropod prisms are not so prominent, consisting of either calcite or aragonite, as identified in X-ray analyses. Bandel (1990) recognized in representatives of this class a number of transitions, for instance, from acicular fibrous prismatic structures to simple lamellar, crossed-lamellar, structures; from homogeneous to acicular crystallites and spherulitic columns; from composite prismatic to crossed-lamellar, etc. Other arrangements are to be found in gastropodes, for example, helical, scaly, dendritic, structures. In monoplacophorans, *Neopilina hyalina* (Weiner and Addadi, 1997) and *Micropilina arntzi* (Cruz et al., 2003), both prismatic and nacreous layers are aragonitic.

2.2.2. Crossed-lamellar structures

This is considered the most frequent shell arrangement, found in classes Gastropoda, Bivalvia, Scaphopoda and in the Polyplacophora *Chiton*. It consists of layers of fine prismatic or sometimes lath like, aragonitic crystals that interdigitate and cross along opposite directions, at variable angles, along different layers. Equivalent crossed structures of calcitic nature are referred to as foliated layers, which have been reported in fossil specimens of oysters and scallops by Runnegar (1984) and in several gastropods by Taylor and Reid (1990).

A general scheme of crossed-lamellar layer (CLL) organization is illustrated in Fig. 2 (Reprinted, with permission, from Dauphin et al., 2003b. *Copyright (2009) by EDP Sciences*). The larger CLL units, known as first order lamellae, are comprised of successively smaller bundles of elongate prismatic units, known as the second, third, forth, up to sixth order. Particularly well-formed crossed-lamellar layers are aragonitic, according to several authors (Bøggild, 1930; Haas, 1972; Dauphin and Denis, 2000). The first order lamellae pile up in layers, however, keeping their main axes rotated at a fixed angle, more frequently at 45–60°, along consecutive layers. As a result, this complex arrangement can exhibit various aspects, according to the observation plane. Such construction tends to impose difficult propagation of a crack wave in a given direction in the shell (Currey, 1988).

A bulky CLL is present in the shell of *Strombus gigas*, similar to "ceramic plywood", which results in a high fracture toughness (Kamat et al., 2000). Yet, other substructures of crossed-lamellar layers are common in Gastropoda (Bandel, 1990; Taylor and Reid, 1990).

Two main arrangements are possible. More frequently, the crystals intersect at 45–60°, as found in several gastropods (Fig. 3A), or the crystals cross at right angles, forming a square grid, as seen in *Conus virgo* (see Simkiss and Wilbur, 1989) and *Pomacea lineata* (Fig. 3B). Scaphopoda have a very prominent aragonitic, complex, crossed-lamellar layer (Fig. 3C and D). This arrangement (CCL) has already been demonstrated by Shimek and Steiner (1997) and by Reynolds and Okusu (1999). Reynolds (2002, Fig. 7) described the existence of two (unequal) CCLs in a shell of *Dentalium laqueatum*. Carter (1990b) listed up to eight varieties of crossed-lamellated microstructures that occur in molluscs. The obliquely crossing CLL, quite prominent in Scaphopoda shells, may account to about half the thickness of their walls, as is the case in *Dentalium* and *Coccodentalium*, Fig. 3C and D, respectively. Alzuria (1985) described "acicular" prisms in *D. vulgare*. Crystals in shells of gastropods *P. cubensis* and *A. fulica* form lozenges, with complementary angles of 60° and 120°, whereas in another gastropod, ill-shaped elongate crystals are arranged in a rather loose packing (Fig. 3E).

2.2.3. Nacreous structures

This is the innermost furrow of the shell, always aragonitic in nature, exclusive to Mollusca, found in bivalves, Gastropods and in the septal chambers of Cephalopod *Nautilus*. Nacre crystals are always aragonitic, laminated, usually presenting sharp edges. The crystals are about 500 nm thick, and they form stacks along a fixed spacing of some 30 nm, filled with biological matter (Addadi et al., 2006). Two arrangements are known: the sheet nacre model of Bivalvia and Cephalopoda, in which the individual tablet-like crystals are slightly displaced along subsequent rows, mimicking a "brick-and-mortar wall" when in profile view; and the "columnar stacking" model, characteristic of Gastropoda (Watabe, 1988). Accordingly, the vertical piling-up of crystals in these shells promotes the formation of columns or pyramids. The regular interspacing of crystals with the organic matrix builds up a rather strong material, whose physical properties – high tensile strength, compressive strength and bending strength – surpass those of a number of others. Mechanical properties of different molluscs shell components were determined by Currey (1988); of these, nacre ranks first. Very recent studies of Bezares et al. (2008) on shell biomineralization in *Haliotis rufescens* relate its mechanical properties to the presence of chitin in the organic framework of the matrix. These authors used an extensive list of immunochemical and cytochemical procedures, combined with atomic force and

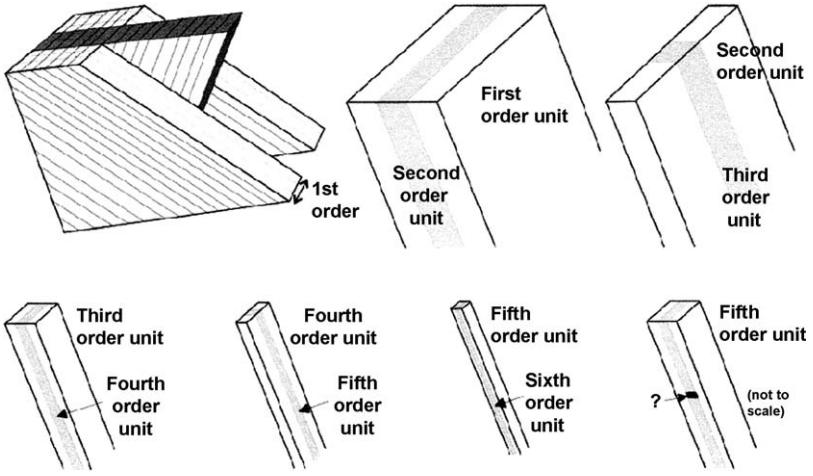

Fig. 2. Schematic drawing to illustrate organization of the crossed-lamellar layer (CLL) in shell of *Concholepas concholepas* (Gastropoda). Five levels of crystalline arrangements are recognized: the largest blocks, or 1st order lamellae, orientate at about 80°, relative to one another. Each lamella is made up of successively smaller units, down to the individual rod-like crystals, which represent the sixth order units (from Dauphin et al., 2003b). Permission of ELS-OXF L.Gould@elsevier.com.

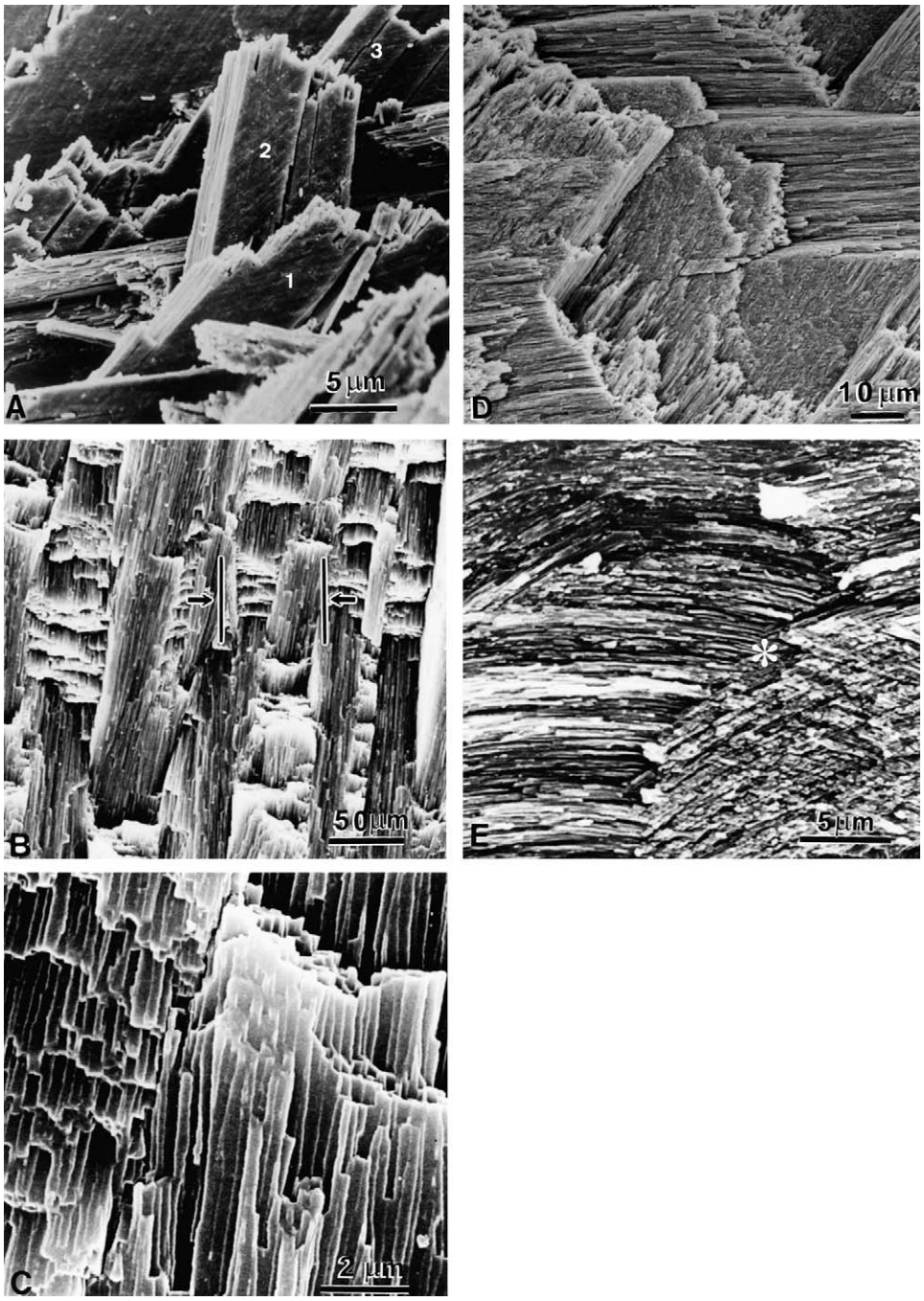

Fig. 3. SEM images of different crossed lamellar layers (CLL) occurring in shells of Gastropoda (A, B and C) and Scaphopoda (D and E). (A) Transversely fractured, hand polished shell of a freshwater pulmonate gastropod, in which consecutive layers of first order lamellae (1, 2, 3) are rotated at angles of about 30°. These lamellae are neatly formed by needle-like prismatic subunits. (B) *Pomacea lineata* CLL. The plate-like crystals pile up in columns about 50 μm thick, with an orthogonal arrangement. (C) Shows elongate, lath like, irregular, thin prisms from a CLL of *Achatina fulica* (Gastropoda). (D) Transversely fractured, hand polished shell of *Dentalium* sp., showing superimposed first order lamellae, obliquely oriented at about 60° relative to each other; this layer forms the bulk of the shell's wall. (E) Shell of *Coccodentalium* sp., in a transverse fracture. Thinner lamellar elements are less distinct; they intersect in arcs at about 120°, so as to form lozenge patterns (*). The individual prisms are unclear (Refer also to Fig. 11G).

scanning microscopies, to obtain a "molecular mapping" of the individual nacre platelet. A comparative study of the two distinctive arrangements, their microstructures and mode of formation, is presented by Wise (1970). These various depositional arrays seem related to the shell calcification mode and would represent useful criteria to studies on phylogeny of the Mollusca.

Axes *a* and *b* of the aragonitic tabular crystals coincide with the depositional direction in the shell, i.e., parallel to the outer surface of the shell. Their smooth surface – "mother of pearl" – gives a characteristic luster to many bivalve shells, due to light diffraction in the micro-laminate crystals (Tan et al., 2004). The outstanding properties of the nacreous layer are related to the insoluble biological matrix, known to be consisted of a chitin–protein complex that would guide the mineral deposition (Levi-Kalisman et al., 2001; Weiss and Schönitzer, 2006). The same evidence was obtained by Cartwright and Checa (2007), who identified that the matrix contains β-chitin molecules, possibly in a liquid-crystal phase, plus silk-fibroin and some glycoproteins, originated in the extrapallial liquid. These macromolecules bind and stabilize the chitin layer, forming the membrane, a fibrous composite. Then, the

mineral phase, calcium carbonate, occupies the space between the interlamellar sheets. Upon crystallization, a composite material of outstanding mechanical properties is obtained (Song et al., 2003; Cartwright and Checa, 2007). This biological layer extends along the surfaces of the individual crystals (interlamellar sheets) and between the individual crystals (inter-crystalline sheets). Weiss et al. (2002b) showed that calcium carbonate is deposited upon this organic framework, initially in the amorphous phase and subsequently converted to crystalline aragonite. Nassif et al. (2005) documented *in situ* this crystallization process, using a sectioned nacre platelet of *Haliotis laevigata*, originally coated with amorphous $CaCO_3$ (ACC). Following irradiation of high energy electron beams (200 and 400 keV) in the HVEM, a phase transformation of amorphous to crystalline nacre could be documented. The application of selected structural techniques, such as cryo-sectioning for transmission electron microscopy (Levi-Kalisman et al., 2001); high resolution TEM (Nassif et al., 2005); atomic force microscopy (AFM) (Giles et al., 1995; Sikes et al., 1998; Dauphin et al., 2003b) and X-ray diffraction methods (Checa and Rodriguez-Navarro, 2005) has considerably contributed to a better characterization of nacre as a biomineral, at a nanoscale dimension (Rousseau et al., 2005). Hou and Feng (2003) investigated the interface between aragonite tablets of *M. edulis* and the intervening organic matrix, using chemical and ion-milling etching methods: they concluded that both mineral bridges and heteroepitaxial phenomena are involved in the growth of nacre. In either case, it seems that the formation of the structural (biologic) matrix containing β-chitin, precedes the crystal nucleation, which involves the participation of silk-fibroin and acidic macromolecules.

A nacreous layer is apparently absent from Scaphopoda and Polyplacophora shells. In Gastropoda, nacre is of columnar type, comprised of small crystalline units, "stacked-up" in pyramids (Wise, Jr., S.W., 1970). The typical "brick-wall" arrangement as found in shells of Cephalopoda and Bivalvia is illustrated in Fig. 4A. At higher magnification (Fig. 4B and C), the surface of the crystals seems rough, likely representing residues of the interlamellar matrix. A quite distinct pattern of nacreous layer was described by Cruz et al. (2003), in the shell of monoplacophoran *M. arntzi*. Field emission TEM images also show rough surface, and electron diffractograms confirmed the aragonitic nature of nacre. Other interesting microstructures of this shell require further identification.

Addadi et al. (2006) recently proposed a new "working model" for the nacreous layer growth in bivalves and cephalopods, which involves the following steps: first, the matrix is assembled, which is followed by the deposition of a transient amorphous calcium carbonate in colloidal form; then, the controlled nucleation of individual aragonite platelets upon the matrix occurs. Thickening of the deposit is most prominent along the *c*-axis (vertical direction). This way, hydrophobic silk proteins are pushed sideways to prevent from incorporating into the aragonitic structure. Comparative studies on nacreous layer arrangement and formation in different molluscs were carried out by Wise (1970), who correlated it with ecological adaptations; the author claims the usefulness of such details for studies on Mollusc phylogeny. The nacreous layer formation, according to Cartwright and Checa (2007), begins with chitin molecules, secreted in the extrapallial space, that join to form sheets or very long liquid-crystal chains, whose diameter is around 20–30 nm. These chains form a discontinuous sheet or mesh of β-chitin, with which glycoproteins and silk-fibroin molecules associate. Calcium carbonate ions are then deposited upon this chitinous mesh. Formed crystals are likely to have defects, such as screw or edge dislocations, that may guide the mineral deposition. In Gastropoda, the nacre crystallites pile up into columns, vertically aligned,

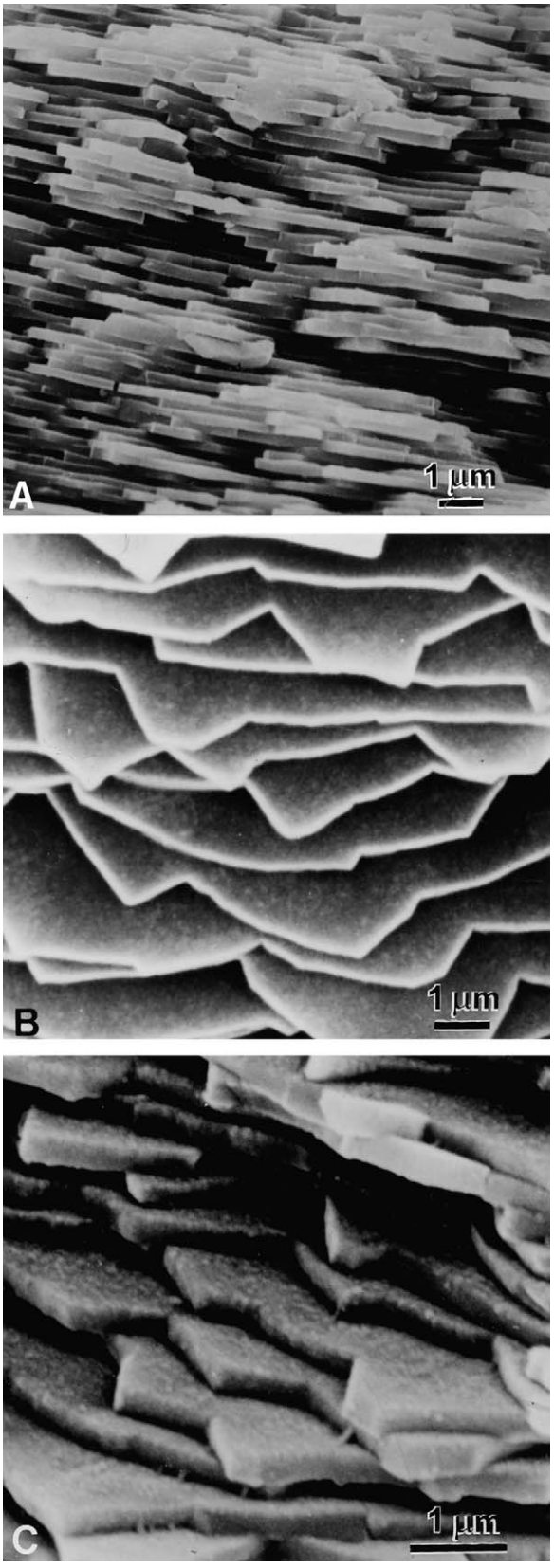

Fig. 4. Nacreous layer of the bivalve, *Anodontites trapezialis*. (A) In a transverse fracture, the nacre shows the typical "brick-wall" arrangement of stacked plate-like crystals. Note the uniform thickness of crystals, about 0.5 μm. In oblique views (B and C), the crystals seem foliated, with polygonal edges. (C) This enlarged view demonstrates that the surfaces of the tablets are rough, with irregular patches, likely representing residues of the interlamellar biological matrix.

whereas in Bivalvia, they are slightly displaced along contiguous rows, to assume the brick and wall arrangement. Briefly, these authors compare aragonite crystals to a "mineral that incorporates organic fibers" and the biological membrane to a "composite of chitin crystals embedded in a proteinaceous matrix".

Shells of cephalopod *Nautilus pompilius* consist of a nacreous layer, externally covered with an even harder material, described by Mitchell and Phakey (1995) as the porcellaneous outer layer that has a granular structure (also referred to as a spherulitic prismatic layer). A periostracum covers the shell surface. Nudelman et al. (2006) demonstrated that the nacre of this same species is very thick, comprising hundreds of stacks of layered aragonitic crystals. The complete shell decalcification provided a clear view of the hexagonal arrangement of the biological matrix around the aragonite plates (intertabular matrix). Histochemical and immunolabelling studies allowed mapping four specific functional zones under the surface of each platelet, which would correspond to the successive stages of crystal development. The experimental success of these studies is attributable to the decalcification of the samples in ion exchange resin to avoid the conventional use of EDTA.

Recently, Dauphin et al. (2008) identified a transitional layer between the calcitic prismatic and the nacreous layers, in shells of *P. margaritifera*, a species of "pearl oyster". The interface between the two quite distinct layers would consist in a very thin stratum (less than 20 μm thick) of a "fibrous aragonite" that can be characterized neither as aragonite nor as calcite. This is resolvable only with AFM. A combination of selected structural and spectroscopic techniques was used in that investigation (micro-X-ray absorption; FTIR; confocal microscopy and AFM), in addition to SEM, that allowed the precise mapping of elemental locations in this reduced (mineralizing) area.

Another advance in the understanding of nacre formation is provided by Bezares et al. (2008), who used a wide spectrum of methodologies, including fluorescence microscopy, enzymatic digestion, immunolabelling, amino acid analysis, the tapping operational mode in AFM and SEM. As a result, it was possible to provide a macromolecular mapping of the interlamellar layer for a single aragonite platelet having nano-dimensions, and determine the mechanical forces related to the chitin fibers that represent up to 6.9% of the insoluble framework. This study confirms and extends previous results of Nudelman et al. (2006): it allowed the identification of structural chitin and specific sites of other macromolecular groups within each nacre tablet of aragonite.

2.2.4. Homogeneous structures

This microstructural category – the HOM structure – according to Carter (1980a) would form various deposits or layers of fine grained material, whose diameter is less than 5 μm, of uncertain mineralogical characterization. Such aragonitic or calcitic particles look homogeneous under SEM and they may occur at specific regions (Chateigner et al., 2000; Kobayashi and Samata, 2006; other examples in Watabe, 1988). In scaphopod *Coccodentalium*, the outermost longitudinal ribs of the shell seem to be filled with such finely structured mineral, as detectable in SEM, in cross-fractured shells.

2.2.5. Spherulitic structures

Spherulites are aggregates of needle-like or foliated crystals that, radiating from a common center, assume a mushroom-shaped or spherical volume; they are frequently found in shells of Bivalvia and Gastropoda, usually linked with growth or regenerating steps. In Cephalopoda, spherulites were reported in *Nautilus macromphalus* (Meenakshi et al., 1974), *Cepea nemoralis* (Watabe, 1981) and *N. pompilius* (Addadi and Weiner, 1992). These aggregates may not constitute a compact layer, unless under competition growth, when they form a spherulitic prismatic layer. Meenakshi et al. (1974) demonstrated compact spherulitic prismatic layers formed under experimental conditions in shells of *Nautilus*. The prisms grew associated with an organic membrane, completing the layer within 30 days. Checa (2000) studied biomineralization of the periostracum in Unionidae bivalve shells that also begins in association with fibrous spherulites, promoting the formation of both prismatic and nacreous layers. The morphological data were complemented with polarization microscopy and X-ray texture analyses. Important data on shell formation and organization of microstructures of bivalves are further provided in a series of subsequent studies by Checa and collaborators (Checa and Rodriguez-Navarro, 2001, 2005; Checa et al., 2005, 2006).

In *A. fulica* (Gastropoda), spherulites occur in close relation to a smooth (biological) membrane. At first, spindle-shaped crystals are found, that seemingly join together at one extremity to assume a stellate aggregate, then thicken and originate solid crystals (Fig. 5A and B). Involvement of the organic membrane is clearly documented (arrowed, Fig. 5A).

Disk-shaped deposits of calcium carbonate frequently associated with organic matter occur on some nacreous surfaces, such as in *Pinctada* (Wada; see Wilbur, 1972); they might correspond to sites of crystals nucleation and growth. Similar images are found for instance on the periostracal inner surface of bivalve *A. trapezialis*, where circular patches of mineralized/mineralizing material are seen (Fig. 5C); their diameters (5–10 μm) match those of the aragonitic "banded" prisms, shown in the profile in Fig. 5D.

Early studies on the formation and growth of prisms were carried out by Nakahara and Bevelander (1971), using thin sectioned material and TEM. The authors concluded that the formation of both nacreous and the prismatic layers in the shell of *P. radiata* are very similar. Calcitic prisms and aragonitic nacre seem to have a common origin within the proximal region of the mantle fold, in the pallial space. The essential point is that synthesis takes place in a defined and restricted mineralizing compartment; in shells, this is limited by the periostracum and the mantle epithelium. Crystallization will occur only after a supersaturated solution is achieved there and crystal nucleation starts.

Investigations on shell structure and composition are essential for complete clarification of the biological phenomena involved in shell formation, growth mechanisms and biomineralization (Weiner and Dove, 2003). This subject has been thoroughly addressed in several excellent reviews: Wilbur (1972); Lowenstam and Weiner (1989); Simkiss and Wilbur (1989). Important recent researches focus on the direct involvement of biological macromolecules in the biomineral assembly: Addadi and Weiner (1992); Addadi et al. (2001, 2006); Nudelman et al. (2006); Marie et al. (2007); Marin and Luquet (2007).

According to Checa (2000), the inner face of the periostracum of different Unionidae bivalves is directly involved in the synthesis of the prismatic layer. Mineralization initiates there, from fibrous spherulites, which grow towards the shell interior and by competition aggregate into prismatic crystals. These studies were supported by texture analyses and careful polarization microscopy methods.

2.3. Biological components of the shell

2.3.1. The shell matrix

The mineral phase of the mollusc shell is intimately associated with a biological material, or matrix, that binds the crystals together from their early stages of assembly, in both prismatic and nacreous layers. This biological component represents less than 5% of the entire shell volume (Marxen et al., 1998; Marin and Luquet, 2004; Dauphin, 2006); however, it is an integral part of the shell

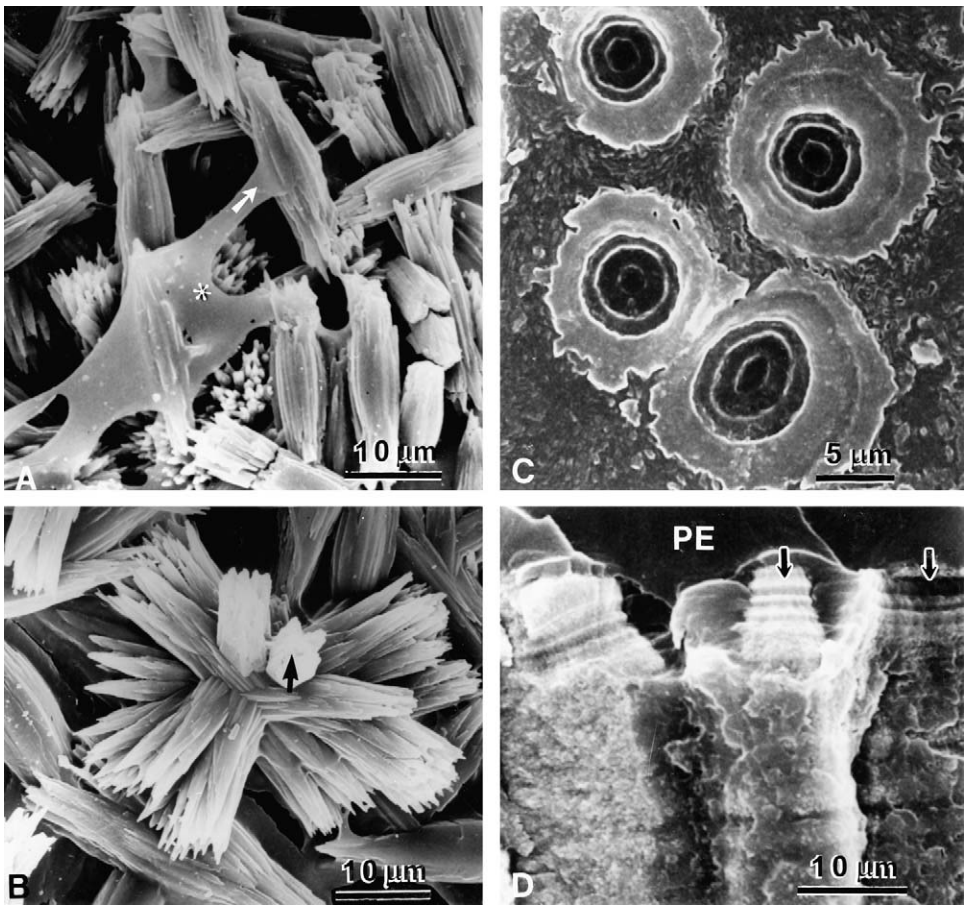

Fig. 5. Spherulitic structures that occur in *Achatina fulica* (A and B); and *Anodontites trapezialis* (C and D). (A) Clusters collected from the surface of the columella. At this early stage of development, spindle-shaped crystallites (arrowed) make close contact with a smooth, organic membrane (*). In a more advanced growth stage (B), crystalline aggregates take on a radial distribution, with thickened crystals (central part, arrowed). (C) Concentric spherulitic patches that occur under the surface of the periostracum of *A. trapezialis*. The central region of each unit is depressed, from where incipient prisms likely originate. In (D), vertical fracture passing through a similar area as in (C), illustrates the contact region between the homogeneous periostracum (PE) and the growing prisms (arrowed). The apical portion of prisms has neat transverse striations; downwards, a rough matrix covers the surface of all prisms.

and is responsible for crystal nucleation, growth and physical properties. Therefore, knowing how this is achieved is extremely important to understand the whole mineralization process. Levi-Kalisman et al. (2001) examined vitrified sections of the matrix of the bivalve *Atrina*, at high resolution TEM. The presence of β-chitin was clear, forming a highly ordered periodic arrangement; a silk-gel phase is found between these sheets. This model is reproduced here, in Fig. 6 (from Levi-Kalisman et al. (2001); *with permission of Elsevier*) and demonstrated a layering of the organic matrix within which mineralization could take place. The organic matrix is formed by β-chitin, silk-like proteins and acidic glycoproteins, rich in aspartic acid. These results contrast with the pioneer images of "conchiolin" obtained in dry samples by Ch. Grégoire (for instance, in Grégoire, 1960, 1972, 1974).

A fraction of biological material is also present in the periostracum and the ligament of bivalves (see below). Therefore, both are considered only partly mineralized components of the shell.

The matrix has been frequently investigated. Two fractions are present, one is the (water)-soluble fraction, and the other is the insoluble component. Although convenient, this solubility criterion is questionable, as both fractions share some common features in their amino acid sequences. Structural aspects of the insoluble fraction have been carefully studied by transmission and scanning

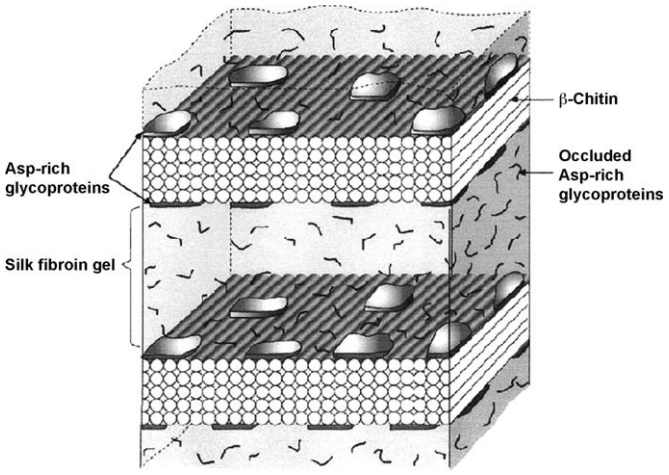

Fig. 6. Three-dimensional model for the biological matrix of nacre from *A. serrata*, as proposed by Levi-Kalisman et al. (2001). In this model, based on cryo-microscopy results of demineralized samples, the matrix would consist mainly of layered β-chitin fibrils interspaced with silk-fibroin gel layers. The surfaces of the chitin layers would be in contact with a "discontinuous" covering of aspartic acid-rich glycoproteins, embedded in the silk-gel of fibroin (from Levi-Kalisman et al., 2001). By Permission of Elsevier/Copyright Clearance Center.

electron microscopy; it forms a distinct envelope around the crystals, showing variable patterns (Grégoire, 1961). It is essentially inter-crystalline, and acts as the framework upon which crystals are deposited. Therefore, the dissolution of the crystalline matter of the shell allows not only a clear three-dimensional view of the insoluble matrix, but also a means of its biochemical characterization (Tong et al., 2002; Dauphin et al., 2003a,b). The matrix basically contains proteins, carbohydrates, polysaccharides and lipids. The soluble fraction is essentially associated with the surface of the insoluble and structured matrix, and also found within the crystals (Tong et al., 2002).

The insoluble matrix isolated from fully decalcified shells of two gastropods, *A. fulica* and *P. cubensis*, respectively, Fig. 7A and B, as examined in the light microscope, demonstrates the presence of filaments arranged in a reticulate pattern. The fibrillar system gave a positive reaction of carbohydrates, using the conventional PAS method, being unreactive in the controls; at this low magnification, it was not possible to distinguish whether the filaments could correspond to collagen-like fibrils. Matrices from bivalve *A. trapezialis*, isolated, respectively, from the nacreous layer (Fig. 7C); and from the prismatic layer (Fig. 7D), following complete shell demineralization in EDTA, also demonstrate fine periodicities (about 10–15 nm thick) embedded in the membrane (Fig. 7C), that likely correspond to the framework of chitin fibrils.

Similar "beads" are also recognized in the isolated prismatic matrices that form a quite structured "honeycomb" arrangement (Fig. 7D). Several repeat bandings can also be identified in these "molds" of the dissolved aragonitic prisms. Tong et al. (2002) and Checa et al. (2005) had previously demonstrated these unusually thick interprismatic membranes in other molluscs shells. The mineral deposition dynamics and the biological and chemical reactions underlying it have not been completely explained. Recent studies by Cartwright and Checa (2007) emphasize the complexity of the phenomena involved, of biological and physical–chemical nature. The matrix is present between each crystalline layer and also within the crystals, comprised of crystalline subunits (Grégoire, 1961; Checa and Rodriguez-Navarro, 2001; Tong et al., 2002; Cartwright and Checa, 2007).

2.3.2. Periostracum

The periostracum is the outermost, protective covering of mollusc shells; it is essentially organic, proteinic, but in part mineralized and it is also involved in shell formation. For certain, a periostracum occurs in Bivalvia and in Gastropoda. Its presence in

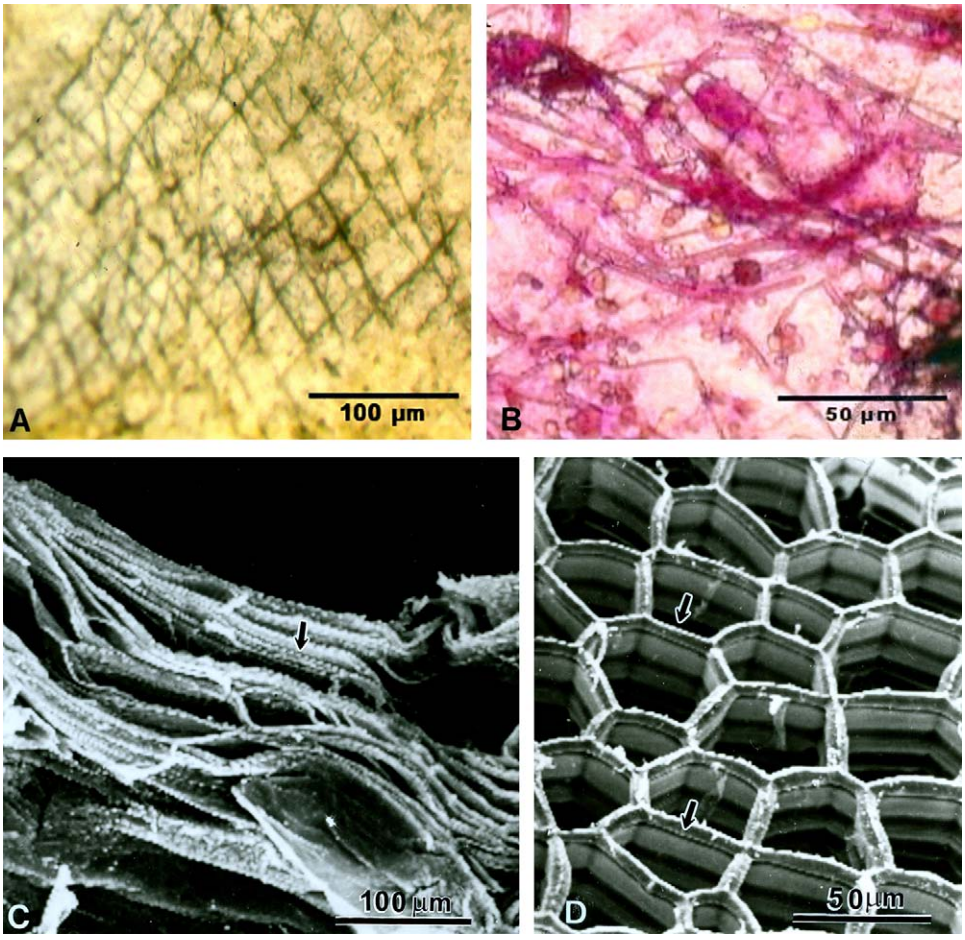

Fig. 7. Insoluble fraction of biological matrices isolated from shells of two gastropods and one bivalve, following complete dissolution of their crystalline phase. (A) *Achatina fulica* (terrestrial gastropod): a reticulate organization is seen, due to obliquely crossing, thin striations. Light microscopy, unstained preparation. (B) *Physa cubensis* (freshwater gastropod). Similar preparation as in (A), followed by staining in the periodate-Schiff reagent (PAS). Light microscopy. Reactive sites correspond to organic matrix fibrils, randomly distributed within the pellicle. (C and D) SEM images of the insoluble matrix from *A. trapezialis* (freshwater bivalve). Shell fragments were fully demineralized in 8% EDTA for several days, extensively washed in water and fixed with OsO_4, followed by impregnation with 1% tannin, dehydrated, critical point dried and gold sputtered. (C) Profile view of the nacreous layer matrix, that is somewhat folded; particulate structures are seen throughout the folds (arrowed), very likely representing the chitin scaffold. (D) The prismatic layer matrix, similarly prepared, shows a typical honeycomb-grid organization. Note periodic bands within every compartment, which might correspond to imprints of growth steps of the (dissolved) prisms. Strings of beads are also apparent along the various levels within each hexagonal unit (arrows). Zeiss SEM, 15 kV. (*) (B) from De Paula (2006).

Scaphopoda is recognized by some authors (Haas, 1972; Alzuria, 1985), but it is still doubtful to others (see Reynolds, 2002). Crystal formation in the absence of a periostracum – thin as it may be, would require a conceptual revision of its effective role. In Aplacophora and Polyplacophora, the true periostracum would be substituted for a kind of cuticular structure (see Watabe, 1984); in *Nautilus*, a 1–5 μm thick, sometimes iridescent, periostracum is present and provided with holes.

The periostracum results from the activity of special cells located within the periostracal groove, at the mantle edge. The formation process varies according to the taxon under consideration (Jones and Saleuddin, 1978; Saleuddin and Petit, 1983). Fig. 8 is from the study of Jones and Saleuddin (1978) (Fig. 1, *Reproduced with permission, from NRC Research Press*). It illustrates elements involved in the periostracum synthesis in *Physa* spp.: specialized cells opening at the periostracal groove secrete lamellar units that are transported to the outer surface of the groove, where they fuse together and contribute to the extracellular periostracal lamellae; mucus and other secretion materials are also produced by different cell types in the groove. Tall mantle edge gland cells from the dorsal epithelium thicken the forming periostracum, other epithelial cells being responsible for initializing the calcium deposition. More important than its protective function is the role the periostracum plays in organizing shell layers, acting as a matrix, in particular, for the prismatic layer (Watabe, 1984, 1988; Checa, 2000).

The periostracum is essentially composed of tanned fibrous proteins, carbohydrates and lipid. 3-4-Dihydroxyphenyl alanine (DOPA) is the possible sclerotization agent. The chemical composition of this layer has been investigated by, among others, Meenakshi et al. (1969): about 40% of the total amino acids in the periostracum are glycin, followed by tyrosin, which represents about 15%. Some low percentage of inorganic ions (sulphur, iron, lead and cadmium) has also been reported to occur (Watabe, 1984). The actual composition varies anyway, according to environmental conditions.

Ultrastructural and cytochemical studies on the periostracum forming tissue have been described for *Macrocallista maculata* (Bevelander and Nakahara, 1967); *Littorina littorea* (Bevelander and Nakahara, 1970); some marine bivalves (Bubel, 1973a,b); and for species of gastropod *Physa* (Jones and Saleuddin, 1978).

There are variations regarding the periostracum structure in different organisms. It usually comprises two layers in freshwater molluscs and a single one in the terrestrial forms, as studied in thin sections by Saleuddin and Petit (1983). The outer layer is proteinaceous; the innermost layer is calcified, frequently brittle.

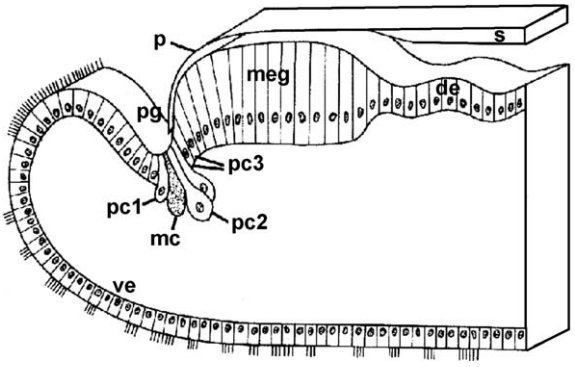

Fig. 8. A diagram reproduced from Jones and Saleuddin (1978), depicts the location of periostracal (p) forming cells (pc1, pc2, pc3) in the periostracal groove (pg), at the mantle edge of *Physa*. The shell (s) emerges above the mantle edge gland (meg). Shell mineralization results from the activity of cells of the thinner dorsal epithelium (de) (from Jones and Saleuddin, 1978). By permission of NRC Research Press.

Folds, corrugations, micro-ridges and spikes may occur on its outer surfaces, for instance, in bivalves (Callil and Mansur, 2005). These authors described in details the multitude of surface projections that occur in juveniles and in adult shells of two species of *Anodontites*.

Fig. 9(A–D) illustrates the general aspects of the periostracum from shells of a bivalve and a gastropod. The broken periostracum (approximately 10 μm thick) may look quite smooth; the fragments are light translucent, sometimes dark-tanned, according to the degree of "sclerotization", due to the content of DOPA (dioxy-phenyl-alanine), cross-linked with the proteins. At higher magnification (Fig. 9B), the periostracum continuity with the structured prismatic matrix is clear. Internal lamellate structures are seen in thin sectioned periostraca of some shells (Jones and Saleuddin, 1978), as also in *P. cubensis*, a freshwater snail (Fig. 9D). The effective participation of the periostracum in the prismatic layer formation seems clear, both in gastropods (Jones and Saleuddin, 1978) and bivalvians. In Unionidae bivalves, growth of prisms is directly associated with spherulits present within the inner face of the periostracum (Checa, 2000).

2.3.3. Ligament of Bivalvia

The ligament is a special system, peculiar to Bivalvia, whose microstructure has not been extensively studied. It is considered a partly organic component of the shell; along with hardened teeth, the ligament forms the hinge system that holds the two shell valves together and allows the shell movements. There are two distinct components: one inner portion that is partly mineralized with aragonite fibers and an outer organic region composed of fibrous glycoprotein (Bevelander and Nakahara, 1969; Grégoire, 1974; Watabe, 1984). There is a matrix, similar to that of the shell, which, in addition, contains methionine and cystein (see Watabe, 1984). Kähler et al. (1976) provided data from X-ray diffraction, chemical analysis and ultrastructural features of the ligament system of *Spisula solidissima*, indicating a content of 62% glycin.

The inner portion of the ligament is also known as "resilium"; its fibrillar character assures the necessary flexibility like a hinge in motion, where the movement direction is controlled by the mineralized teeth. *Mya arenaria* uses the ligament to help the unusual behavior of burrowing, that includes a rocking of the shell, as detailed by Checa and Cadée (1997).

Relatively few information has been available on this system, at the ultrastructural level, since the initial light microscopic studies of Trueman (1950, 1951), who first recognized the two zones. Bevelander and Nakahara (1969) examined in thin sections the inner part of the ligaments of *M. edulis* and *P. radiata*, with emphasis on its formation process. Kähler et al. (1976) studied that of *S. solidissima*, confirming the protein-mineral composition of the system. Marsh et al. (1976) and Marsh and Sass (1980), using electron diffraction (SAED), demonstrated that aragonite fibers are twinned. Scanning electron microscopy investigations by Mano (1980) point to the presence of spherulitic aggregates in the basal part of the hinge system of bivalves *Mercenaria mercenaria* and *Brachidontes exustus*. In *A. trapezialis*, two distinct phases are observed: the mineralized component, comprised of thin aragonitic prisms (Fig. 10A), is easily dissociated by sonication; and the organic component, that is rather compact and reacts strongly with OsO_4 (Fig. 10B). It is also fibrillar in nature and contains small punctures. Isolated fibrils from the mineralized components exhibit Bragg reflections and provide diffractograms that identify its aragonitic nature (Fig. 10C and D). These ligament structures of *A. trapezialis* are very similar to those of *Aetherea elliptica* studied by Grégoire (1974), who also obtained diffractograms from isolated crystals.

A detailed model for the ligament of *Pinctada maxima* is given by Zhang (2007), who analyzed the ultrastructure and light reflectivity of dry and wet samples. The author arrived at a model of

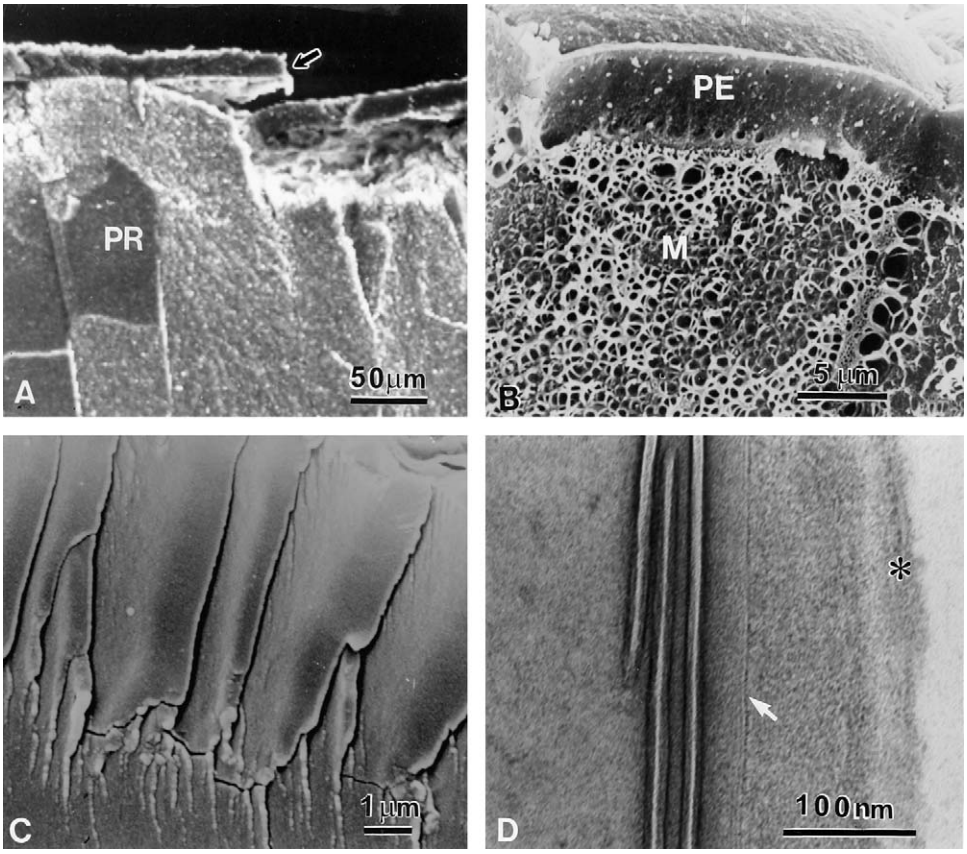

Fig. 9. Periostracal structures. (A–C) SEM views of vertically fractured shells of *A. trapezialis*. Small shell fragments were cleaned by sonication in water, dried and gold sputtered. In (A) the periostracum (arrowed) was partly detached from the prismatic layer (PR). The organic component of the periostracum would correspond to the (less emissive), dark band. (B) Higher magnified view of a periostracal layer (PE), about 5 μm thick, from another shell. The lacelike prismatic matrix (M) extends downwards from this, to envelope the prisms. (C) Folds within a fractured periostracum show a smooth surface. (D) Is a thin-section of an OsO_4 fixed, resin-embedded periostracum of *Physa cubensis* (gastropod); section stained with uranyl acetate/lead citrate. A thin line (arrowed) demarcates two different regions in this periostracum, the left one containing three parallel lamellae. Outer surface of periostracum is to the right side (*). TEM, 160 kV. (D) From De Paula (2006).

lamellate structure, about 35 μm thick; aragonite fibers (ca. 78 nm), are regularly embedded at 127 nm spacing in the protein matrix, in such a way to behave as a photonic crystal. Normal dry ligaments are black, but if wet, they emit a blue structural color, demonstrated through infrared spectroscopy.

3. Shells of Scaphopoda

This is a small class of Mollusca, exclusive of marine, mostly benthonic, habitats. Scaphopoda comprises 1000 species at most; about half is fossil representatives (Reynolds, 2002). Their "tusk-shaped" shells are of reduced size and have two open ends, the anterior end is broader than the distal one, or apex, that is used for water inflow/outflow. Scaphopoda may bear affinities with Bivalvia, according to Fischer-Piette and Franc (1968) and Salvini-Plawen (1980). Ultrastructural information about these molluscs and their shells are relatively scanty, compared to the other classes; however, there is a recent growing interest in these organisms, which are seen as evolutionarily advanced by some investigators.

According to Reynolds (2002), scaphopodans are one of the smallest mollusc classes, although having a significant worldwide distribution. They are "among the least understood molluscs". Also, their body anatomy has been poorly investigated so far (Haas, 1972; Alzuria, 1985; Shimek and Steiner, 1997; Ruthensteiner et al., 2001); and its systematics and classification have not been firmly determined (Salvini-Plawen, 1980; Reynolds and Okusu, 1999).

A classification of Scaphopoda based on shell sculptures has been presented by Emerson (1962), who considered it the "most useful taxonomic criteria". Some points of Emerson classification have been questioned by Palmer (1974). Shimek (1989) proposes a morphometric index for the identification of *Cadulus* species. Reynolds (1997) reviews data on phylogeny from a cladistic approach. SEM has also proved quite useful for studies of scaphopods classification and phylogenesis (Haas, 1972; Reynolds, 2002). Most shells are rather fragile and their surface sculptures, as well as microstructures and number of layers, seem helpful characters for classification and phylogenetic studies (Emerson, 1962; Reynolds and Okusu, 1999). Specimens illustrated here came from 175 m deep, South Atlantic mud (see Table 1).

As a whole, the Scaphopod shell is three-layered, entirely aragonitic. The periostracum may be 1.5 μm thick, according to Haas (1972), although it is frequently worn away, mainly due to the animals burrowing way of life. An outer crystalline prismatic layer (usually very thin) is followed by a thick, complex crossed-lamellar layer. This CLL may have a "regular or irregular structure" (Reynolds and Okusu, 1999). Shimek and Steiner (1997) described an "inner aprismatic layer" lining the shell interior. In Abbot's Handbook on American Sea shells (Abbott, 1974), the classification is based on morphological characters of the shell. Internal ultrastructure of the animals is addressed by a few publications (Shimek and Steiner, 1997; Ruthensteiner et al., 2001; Reynolds, 2002).

SEM shows rich surface ornamentations, as illustrated here. Some shells are shiny, smooth-surfaced, and unstructured, like

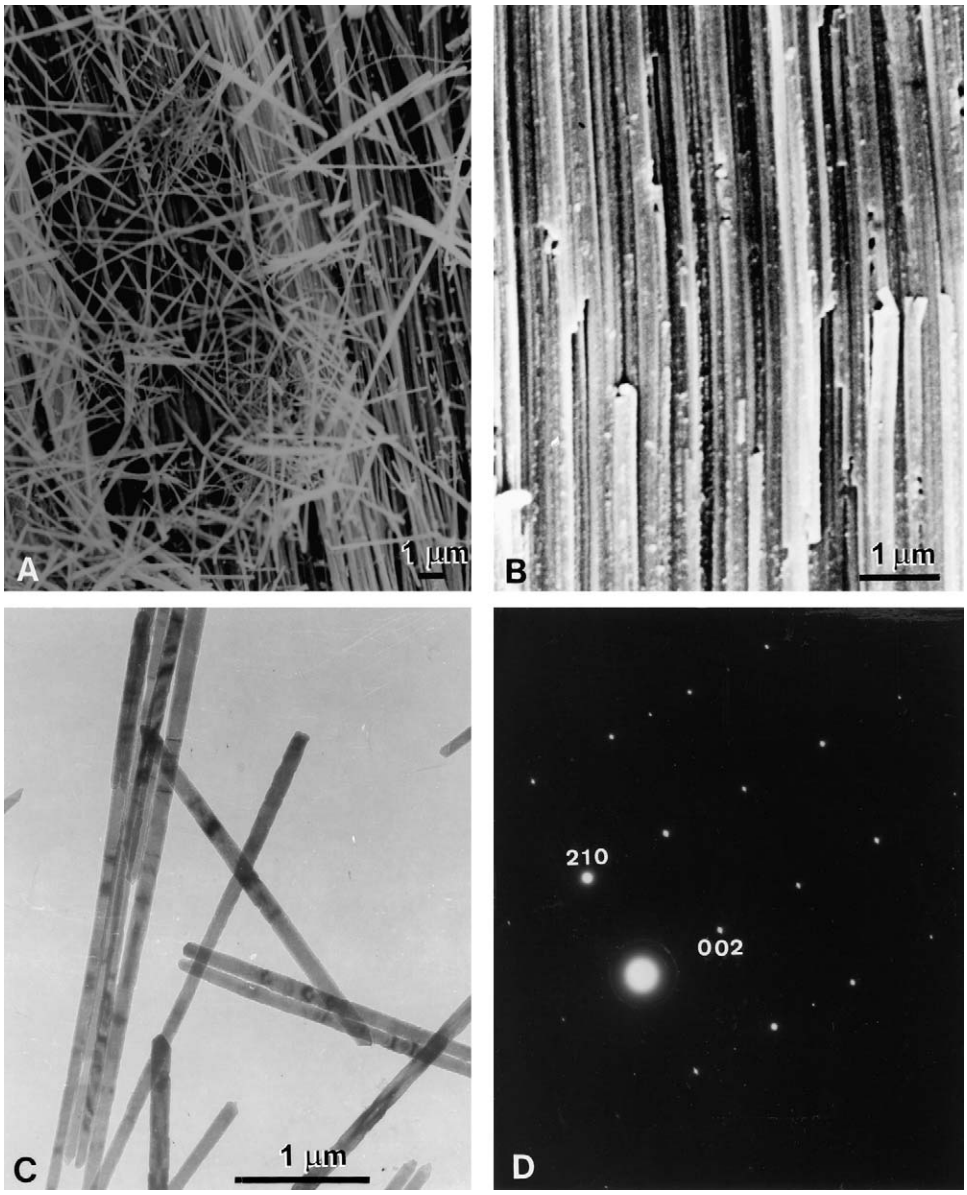

Fig. 10. Hinge ligament of *A. trapezialis*: (A and B) SEM views; (C and D) TEM images. In (A), aragonite needles from the inorganic part of the ligament are shown at low magnification. The crystals were teased apart and gold sputtered. (B) Is a compact bundle of organic fibers, directly impregnated for 24 h. with OsO_4, ethanol dehydrated, critical point dried, then fractured and gold sputtered. (C) Thin fibrous crystals directly isolated by sonication in ethanol and deposited onto a carbon film. Note the diffraction bands along each fiber. (D) Corresponding electron diffraction diagram (SAED), showing the characteristic pattern of aragonite: the distances and the angles between spots (0 0 2) and (2 1 0) identify the crystal parameters of aragonite (orthorhombic system: $a \neq b \neq c$; $\alpha = \beta = \gamma = 90^{\circ}$). TEM, at 200 kV.

Fustiaria sp. (Fig. 11A); others are finely striated, as seen in a (likely) *Plagyoglypta* sp. (Fig. 11B); or a complex system of longitudinal ribs and cross-striations is present, as in *Coccodentalium* sp. (Fig. 11G and H). The tube shape, straight or curved, open at both ends, varies from conical to prismatic. Details of the shell apex are also variable, from a perfect circular opening (Fig. 11I) to others rather elaborate, with slits, notches, etc. (Fig. 11C, D, I, and J). Definitions of sculptures like these are less evident in light microscopic images (see Bøggild, 1930); therefore, further application of SEM can be of great help for their better characterization.

4. Shell and bone—a comparative approach

From several viewpoints, mollusc shell can be compared with bone of vertebrates, for being biomaterials that share important mechanical properties: they are tough and stiff composites, also endowed with mechanical strength, but prone to undergo oriented fractures. These properties have been reviewed in a comprehensive way by Weiner et al. (1999) – for bones; and by Currey (1988, 1999); Kamat et al. (2000); Cortie et al. (2006) – for shells. In both materials, these characteristics result from an intimate association between biological and mineral components, in which the mineral phase develops directly under control of the organism to form unique crystal habits. This characterizes a process of "biologically controlled mineralization", as conceived by Mann, 1983; Weiner and Dove, 2003. In bone, the building blocks are mineralized collagen fibrils arranged in a variety of hierarchical levels, starting with unitary dahllite crystals and collagen molecules; these are packed in tendons, osteons, even spongy and compact bones (Weiner and Wagner, 1998). In bone, collagen type I makes up 70–90% of the non-mineral component, and water amounts to about 15% (for humans). Collagen I is a triple-helix coiled molecule (about 300 nm long × 1.5 nm wide), typically banded at 67 nm

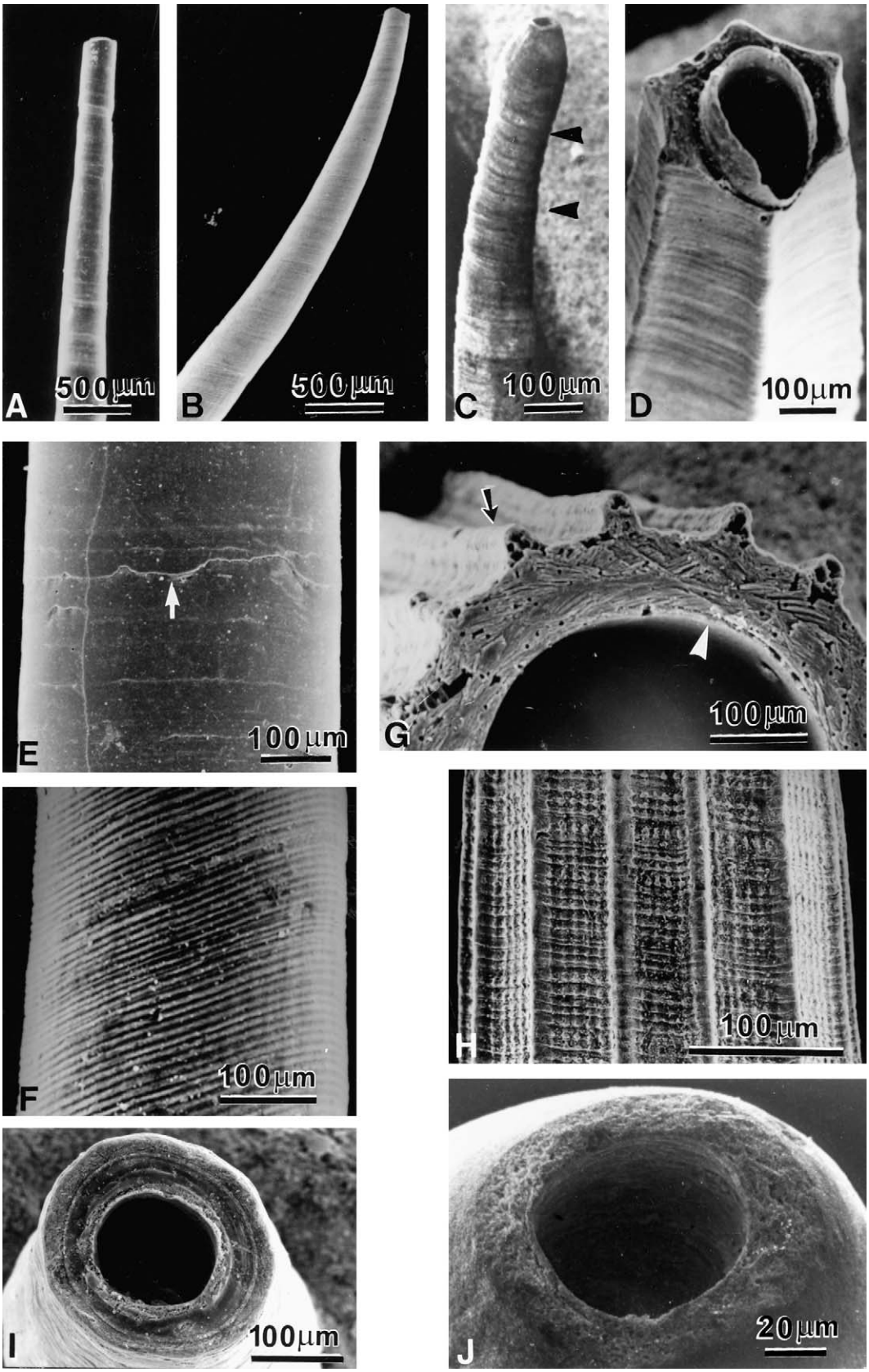

Fig. 11. SEM images of Scaphopoda shells. All specimens were cleaned by sonication, dried, mounted onto the stubs and gold sputtered. (A–D) are low magnification views of apical portions from four different genera, respectively: (A) "*Fustiaria* sensu lato" Palmer (1974); (B) *Plagioglypta* sp.; (C and D) are two as yet unidentified, shells. In *Fustiaria* the shell is almost straight, and has a smooth and shiny outer surface; only sinuous sutures and growth lines are present (see E); (B) *Plagioglypta* sp. presents neat oblique striations likely forming a shallow spiral, all along its surface. Line spacing is at 1 µm, illustrated in (F) and also visible around the shell apex (I). (C) Shows the distal portion of another scaphopodan shell. It has a cylindrical terminal region, somewhat broadened at the sub-apical end; a series of undulations (between arrowheads) follows, behind which the shell shape changes to that of a 6-sided, broad prism. The apex has a circular opening (J). (D) Is another rather voluminous shell – shown at same magnification as in

periods. Other 2–5% of biological matter containing phosphoproteins, glycoprotein, sialo-protein, proteoglycans and some lipid form the matrix that cements together the inorganic phase and admittedly participates in the calcification process (Hoshi et al., 2001).

The mineral phase consists of plate-like crystals of calcium phosphates, mostly dahllite or carbonate–hydroxyapatite (HA)–$Ca_5(PO_4CO_3)_3(OH)$, that are deposited in restricted and specific sites along the collagen fibers. These crystals are continuously reabsorbed and deposited at different rates. X-ray diffraction and high resolution cryo-TEM studies demonstrate that these minute crystals (50–25 nm) also are very thin, about 4–6 nm; low angle X-ray scattering (SAXS) data still gives a smaller value of 1.5–4.0 nm, so HA likely represents the smallest biologically formed crystals (Weiner and Wagner, 1998). Stiffness of bone is very likely related to the amount of HA, to the geometric arrangement and the amount of organic matrix present (Fratzl and Gupta, 2007). In addition to collagen, bone matrix contains other proteins and lipid.

In Mollusc shell, calcium carbonates (aragonite and calcite polymorphs) are interspaced with an organic, hydrated and firmly structured matrix that has been demonstrated to precede crystal nucleation (Veis, 2003).

Nacre has been used as a natural material for bone replacement, with biocompatible, osteoinductive and osteogenic properties (Kim et al., 2002; Pereira-Mouriès et al., 2002a). Thermal decomposition of biological matrices of the two materials is quite different; that of nacre being much more thermally stable than that of bone (Balmain et al., 1999). Despite these differences, both are biological tissues with a crystallization process mediated by a macromolecular matrix. Westbroek and Marin (1998) followed *in vivo*, the interaction between nacre and bone of a female patient, which resulted in the formation of osteoblasts; no evidence of inflammatory process was verified, and nacre had been incorporated into the tissues. The nacreous coating was bioactive, biodegradable and resistant to the propagation of the cracks.

Other recent studies reinforce the compatibility between these two materials, such as the capacity of nacre to induce mineralized tissue formation by osteoblasts (Liao et al., 2002; Berland et al., 2005; Duplat et al., 2007). The results have indicated that nacre implants in the living body provide adequate condition for bone formation (Delattre et al., 1997; Liao et al., 2000; Liao et al., 2002; Milet et al., 2004).

5. Analytical studies

5.1. Fourier transform infrared spectroscopy (FTIR)

Infrared spectroscopy is usually applied in the investigation of the composition of both inorganic and organic materials (Hasse et al., 2000; Wang et al., 2003). It allows the identification of characteristic functional groups in molecules that correspond to specific molecular vibrations (Conley, 1966). In addition, sampling is easy and requires a small amount of materials (about 1 mg). FTIR has also been applied for comparing the organic composition of different molluscan shells (Dauphin, 1999; Dauphin et al., 2008).

5.1.1. Inorganic and organic components

FTIR has proved to be very useful in studies of molluscan shells (Dauphin, 1999; Schladitz et al., 1999; Brugnerotto et al., 2001). With this technique, it has been possible to investigate shell calcification from the embryonic to the adult phase and determine the functional groups involved in the shell composition. Studies on molluscan shell composition using FTIR provide spectra with an excellent spatial resolution that discriminates between carbonate and phosphate groups. The process of shell formation, starting from the embryonic phase in molluscs, is not yet completely understood. The mechanisms involved in shell formation studied by Hasse et al. (2000) using FTIR, established that the organic matrix can be detected at about 60 h and being totally developed after 6 days. The spectrum bands of aragonite were only observed in the adult shells.

It is well known that the nacreous layers of molluscan shells are comprised of aragonite with just a low proportion of calcite. Balmain et al. (1999) and Tan et al. (2004), clearly demonstrated the composition of *Haliotis glabra* through use of FTIR and SEM. This information corroborates previous data of Compere and Bates (1973) on several molluscan shells. Some shells have traces of calcite and a few species essentially have calcite. Vaterite is a rare polymorph (Watabe, 1983). The mineralogy of the crossed-lamellar layer of three bivalves (*Dosinia ponderosa*, *Tridacna* sp., *Cardium* sp.) and of some gastropods (*Cypraea leviathan*, *Phalium granulatum* and *S. gigas*), examined by Dauphin and Denis (2000) using FTIR, showed spectra with strong bands corresponding to aragonite plus some unidentified bands. The nacreous layer of these gastropods has a similar structure to that of *D. ponderosa*.

FTIR analyses of shells from gastropods *P. cubensis*, *A. fulica* and *P. lineata*, indicate only the presence of aragonite (Figs. 12–14, respectively), resulting in similar FTIR spectra for all of them. The differences observed on the absorption peaks can be correlated with the interaction among the organic matrix, inorganic ions and calcium carbonate.

The biogenic crystal growth is controlled by an organic matrix responsible for defining: (a) crystal nucleation; (b) crystal size; (c) crystal orientation; (d) crystal morphological characteristics (Wilbur and Saleuddin, 1983). The use of infrared spectroscopy has identified the functional groups responsible for organic matrix composition in molluscan shells, an important insight to understand the correlation involving the organic matrix and the crystal growth.

FTIR performed with shells of *P. cubensis* (De Paula, 2006) demonstrated that the insoluble organic matrix (Fig. 15) is characterized by bands corresponding to amide I (at 1690 and 1670 cm^{-1}); bands of amide II (at 1553 and 1420 cm^{-1}) and some lower intensity bands probably corresponding to amide III (at 1380 and 1328 cm^{-1}). The 1240 cm^{-1} peak probably corresponds to sulphate absorption. Polysaccharide bands were observed between 1157 and 1000 cm^{-1}. A low intensity band at 1157 cm^{-1} probably corresponds to phosphate. These vibration modes are frequent in the organic composition of other shells (Marxen and Becker, 1997; Pereira-Mouriès et al., 2002b; Dauphin, 2003). Sulphate was usually present in the organic matrix of various other species (Watabe, 1981; Saleuddin and Petit, 1983). Phosphate is also a common component of the prismatic and lamellar layers of gastropod *Concholepas concholepas* (Dauphin et al., 2003b).

Marxen et al. (1998) demonstrated that the insoluble matrix extracted from shells of snail *Biomphalaria glabrata* has a strong protein peak at 1656 cm^{-1} (amide I), and a medium band at 1528 cm^{-1} (amide II). The band at 1228 cm^{-1} was ascribed to

(C). It also is a 6-angled tube in overall shape; the apex contains a secondary tubular structure in eccentric position. Fine transverse striations cover all the 6 outer facets. (E and F) Are enlarged images of outer surfaces, respectively, from (A, *Fustiaria*) and (B, *Plagyoglypta*) shells. (G and H) Shells of *Coccodentalium* sp., in transverse and longitudinal views, respectively. (G) Shows a hand-polished, transverse fracture of a shell near its distal apex. Characteristic longitudinal ribs (black arrow points to one of these) are regularly distributed on the outside. The wall is about 80 μm thick, almost entirely formed by crossed-lamellar crystals. The inner "aprismatic" layer, some 2 μm thick (white arrowhead), is almost undistinct. (H) Shows an enlarged outside view of another *Coccodentalium* specimen, pointing to its complex substructure. The salient longitudinal ribs are equally spaced, at about 50–70 μm. Among these, secondary longitudinal and transverse striations make up a geometric arrangement on surface view. (I and J) Are end-on images of the apical apertures of shells discriminated above, respectively (B) and (C). SEM, 25 kV; (C) and (J), taken with a Zeiss DSM 940 SEM, at 15 kV.

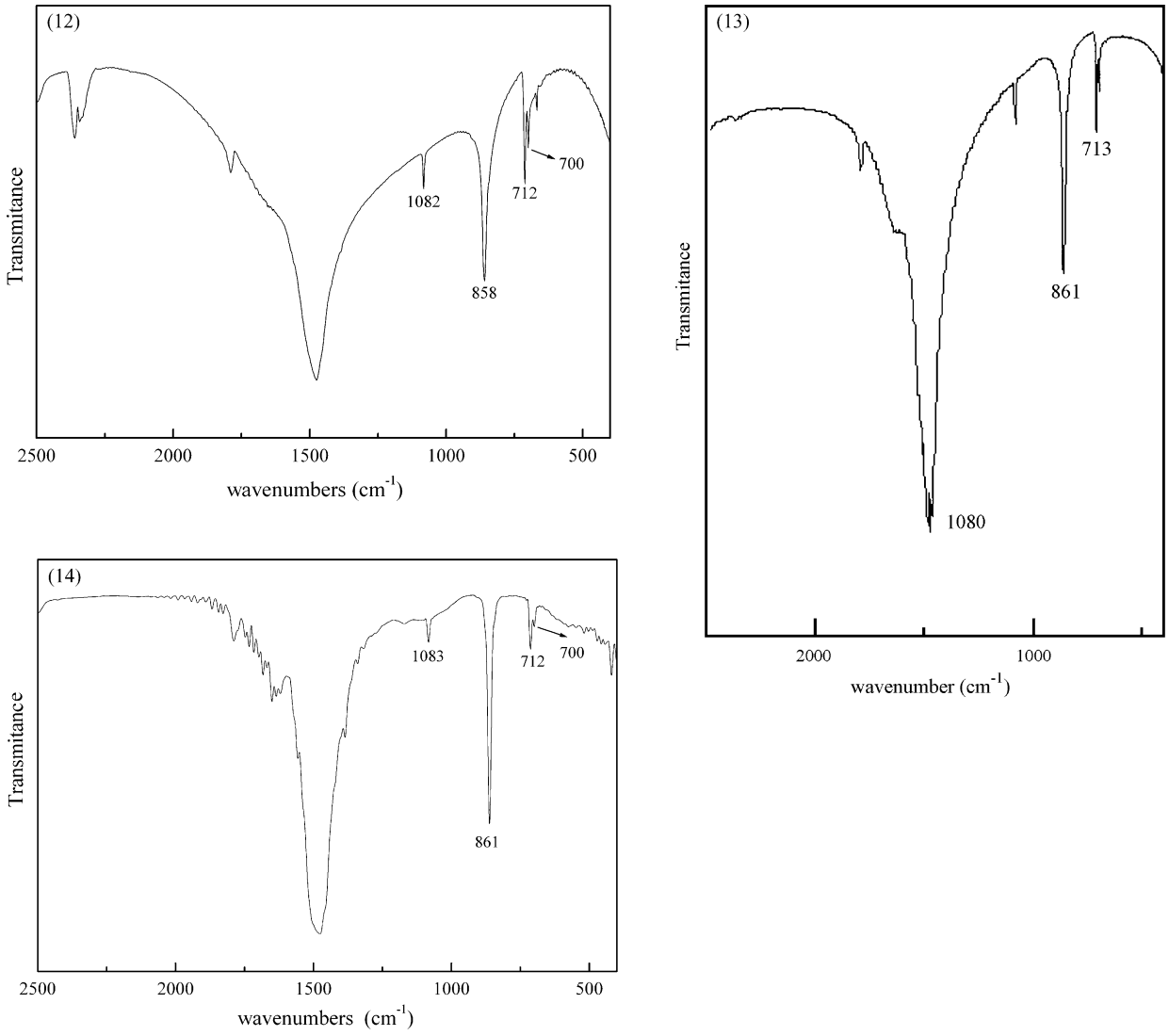

Figs. 12–14. FTIR spectra of samples ground in KBr pellets, of mineral phase extracted from shells of *Physa cubensis* (Fig. 12); *Achatina fulica* (Fig. 13); and *Pomacea lineata* (Fig. 14). The mineral phases are demonstrated by the internal vibration modes of the carbonate ions, ascribed to aragonite characteristic absorption peaks.

sulphate and that at 1073 cm^{-1} to carbohydrates. The presence of chitin was also investigated by these authors, but no peak was obtained.

According to Dauphin and Denis (2000), the mineral components extracted from lamellar layers of bivalves and gastropods are similar, infrared spectra confirming the aragonitic composition, whereas the organic matrices diverge in their organic bands. In addition, analyses from several bivalves showed that the organic matrix of the lamellar layer differs from that of the prismatic layers. Amide I bands are numerous in gastropod shells, but less abundant or absent in bivalve shells. The amide II bands are present only in gastropods. Low content of sulphur, glycoproteins of high molecular weights and strong acidity are common characteristics of soluble organic matrix. Soluble and insoluble matrices of cephalopod *N. macromphalus* L. shell studied by Dauphin (2006) are also distinct. Both matrices have traces of sulphur, bands characteristic of sugars, higher in the soluble fraction.

Lipids are the third component of the biological matrix of biominerals, although analyses dealing with this component in molluscan shells are scarce. Recently, Farre and Dauphin (2009) verified through spectrometry and thin layer chromatography the difference in lipids content between prismatic and nacreous layers

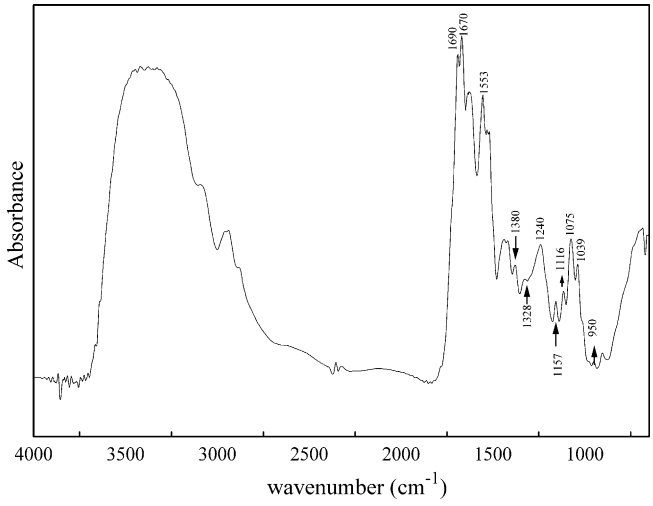

Fig. 15. FTIR spectra of powdered samples ground in KBr pellets, of biological insoluble matrix extracted from *Physa cubensis* shells. There are bands corresponding to amide I, amide II and lower intensity bands associated with the amide III. Smalls peaks nearby 1240 and 1157 cm^{-1} likely correspond to sulphate and phosphate absorptions, respectively.

of *P. nobilis* (Mytiloidea) and *P. margaritifera* (Pterioida, Pteriidae); both organisms contain lipids, but there are compositional differences. The knowledge of the organic composition is crucial to understand the biomineralization process; few information about the action of lipids during this process have been described.

In general, the main features of biological matrices extracted from some mollusc species differ markedly. The organic matrix extracted from the nacreous layer of the oyster *P. maxima*, using two different methods, provided different results (Wilbur, 1964; Pereira-Mouriès et al., 2002b). Further studies and investigations on the characterization of the soluble and insoluble matrices are needed.

5.2. Selected area electron diffraction (SAED)

Electron diffraction is the phenomenon resulting from the interaction between electrons and crystalline materials, producing a pattern of rings or spots that characterize the sample (Glauber and Schomaker, 1953). The diffraction diagram produced by a single crystal provides information about its crystalline structure, lattice parameters and crystal orientation.

A single crystal can be selected and its electron diffraction pattern directly related to the image of the sample. Polycrystalline samples comprised of many unoriented tiny crystals provide a pattern of concentric rings (Hirsch et al., 1965). Both modalities of electron diffraction can easily be carried out in TEM and are extremely useful in the study of molluscan shells.

5.2.1. Electron diffraction

Electron diffraction performed with TEM allows elucidation of the interrelationship among the shape, size, phase of minerals, crystallographic orientation and texture of biominerals in specific locations (Watabe, 1956). This technique has been used by Wilbur (1964) for studying regeneration processes. Results obtained from the several layers of *Helix* shells are typical of aragonite, while crystals resulting from regenerated shells usually show the calcite pattern (Saleuddin, 1971). This transformation, aragonite–calcite, can be associated with the fact that the biological matrix composition of the original shell differs from that of regenerated shell (Saleuddin and Hare, 1970). The advantage of this technique is the possibility to relate the diffractograms directly with the observed region of the sample.

Living organisms are able to deposit a great variety of crystalline materials Molluscs synthesize in their shells about 20 different minerals that have been identified through X-ray diffraction and/or electron diffraction. The structures of shells are extremely diverse (Wilbur, 1964); calcium carbonate growth and polymorphism are affected by different combinations of macromolecules, as experimentally demonstrated by Albeck et al. (1993), Fritz et al. (1994) and Addadi et al. (2001). Several types of $CaCO_3$ crystals are deposited along different locations during growth. Table 2 summarizes the polymorphism of $CaCO_3$ observed in a specific location of various molluscan shells, as demonstrated through electron diffraction. Therefore, the crystallographic analysis is carried out with TEM using electron diffraction to identify the crystal type at the ultrastructural level (Simkiss and Wilbur, 1989).

Crystal orientation may be relatively uniform for a particular layer of a given molluscan shell, but different in another layer of the same organism. In some animals like *Tectus* and *Pinctada*, Simkiss and Wilbur (1989) have demonstrated a correlation between biological matrix and crystals; these shells include the crystal *a* axis aligned with the chitin and the *b* axis aligned with the polypeptide chains.

Morphological results obtained with horizontal sections from nacreous layers of the bivalves *P. martensii* and *Elliptio* complanatus demonstrated that these layers contain polygonal crystals of aragonite with their axes oriented in the same direction (Watabe, 1965). A similar result was found for crystals in the nacreous layers of bivalve *M. edulis*, which presents two types of tablets. Type I has almost the same orientations of *a* or *b* axes, and type II is characterized by a secondary preferred orientation (Hou and Feng, 2003). Although some molluscs have the nacreous layer characterized by a similar crystallographic orientation, divergences have been reported, even for the same species. In some bivalves, for example *Cristaria plicata* and *Hyriopsis cumingii*, the angles between the a axis of adjacent tablets have random crystallographic orientation (Feng et al., 2000a). The nacreous–prismatic interface of gastropod *H. rufescens* described by DiMasi and Sarikaya (2004) is characterized by different relative orientations.

The crystallographic orientation in shells of bivalve *M. edulis* was investigated by Weiss and Schönitzer (2006) and by Feng et al. (2000b). The Laue spots in the diffraction patterns of three adjacent crystals demonstrated that they correspond to single crystals of calcite, having the same three-dimensional orientation. The SAED pattern of the prismatic layer of *C. plicata* shells demonstrated that each region contains crystalline material and a substructure of organic matrix. The intergranular boundary of this layer shows amorphous diffraction rings, thus, demonstrating the presence of organic material, which can possibly influence the crystal growth, direction, spatial orientation and size (Tong et al., 2002).

The SAED patterns obtained via transmission electron microscopy of the species *A. trapezialis* (Fig. 16) and *M. maculata* (Fig. 17) are characteristic of aragonite with orthorhombic unit cell parameters ($a = 4.962$ Å, $b = 7.970$ Å and $c = 5.739$ Å). The crystal directions are $(3, 1, \bar{4})$ for *A. trapezialis* and $(1, \bar{2}, 0)$ for *M. maculata*. These diffraction patterns showed that, although both crystalline phases obtained are characteristic of aragonite, the crystal orientation associated with different molluscan shells are different, suggesting the organic composition of these organisms directly affect the calcium carbonate formation.

5.3. X-ray diffraction (XRD)

Material analysis using diffraction techniques can be performed with neutrons, X-rays or synchrotron light. XRD is one of the most important techniques used for the characterization of materials at the atomic level in Materials Science, Solid State Chemistry (Warren, 1969; Winick and Doniach, 1980) and in studies of protein structure (Von Dreele, 2007).

For further characterization of the sample properties, it is indispensable to apply a method of structural analysis. The Rietveld method (Rietveld, 1969) has been employed to determine the crystalline structures of inorganic materials (Von Dreele, 1999; Toraya, 2000). The structure refinement obtained provides information about symmetry, site occupancies, atomic positions and unit cell (Pokroy et al., 2006). Some free software programs as GSAS (Larson and Von Dreele, 2001; Toby, 2001) or MAUD (Lutterotti et al., 1997) are available for structural refinement analysis.

5.3.1. Diffraction patterns

The X-ray diffraction method has significantly contributed to the development of molecular biology in the characterization of proteins of living organisms (Falini et al., 2002, 2003). The interface between protein and inorganic material provides information about the developmental processes involving calcium carbonate crystallization (Lutts et al., 1960; Weiner and Hood, 1975; Pokroy et al., 2006).

Biogenic minerals occur in more than 40 different types of living organisms. Molluscan calcareous shells have a complex microstructure in which different types of calcium carbonate crystals are

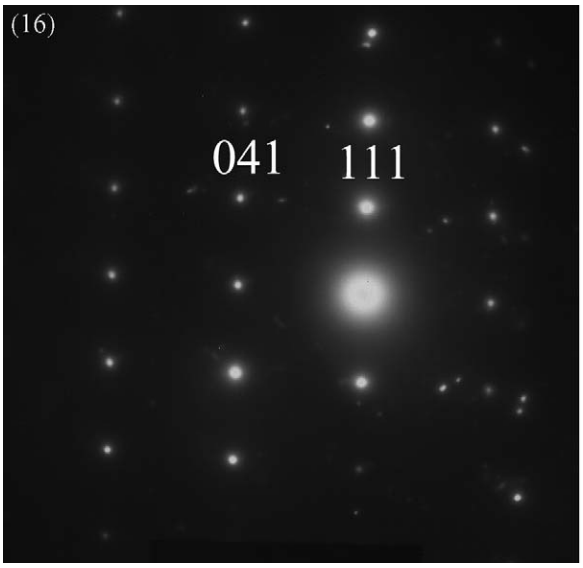

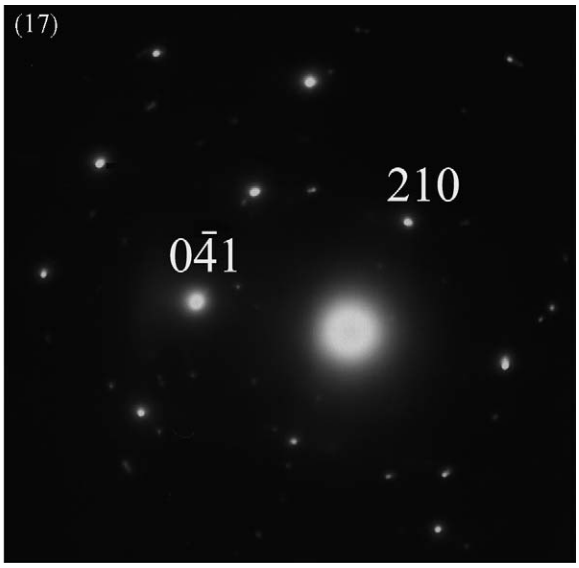

Figs. 16–17. SAED patterns corresponding to aragonite having selected reflections and *d* spacings, respectively for *Anodontites trapezialis*: (0 4 1) (1.88 Å) and (1 1 1) (3.9 Å) (Fig. 16); for *Macrocallista maculata*: (0 $\bar{4}$ 1) (1.88 Å) and (2 1 0) (2.37 Å) (Fig. 17).

deposited (Bøggild, 1930; Lowenstam and Weiner, 1989). X-ray diffraction provides information about mineral identity, thickness, roughness, rate of growth, density and crystallinity. With this method, detailed information can be obtained at high resolution (Checa et al., 2005). Medakovié (2000) also demonstrated that diffraction patterns provide extensive information about the mineralization processes that occur during the shell developmental stages, showing how the calcium carbonate phase is modified from the larval stage to the adult age.

X-ray diffraction spectra showed the occurrence of amorphous calcium carbonate in the embryonic developmental stage. During shell growth, this content decreases whereas the proportion of the aragonite phases increases. Calcite traces were only detected in some organisms (Medakovié et al., 1997). These results indicated that the amorphous calcium carbonate is a precursor phase of aragonite (Marxen et al., 2003). Crystal morphology and polymorphism are intimately correlated with the organic composition during the calcium carbonate crystallization (Watabe, 1984), just as during the regeneration steps (Wilbur and Watabe, 1963; Su et al., 2004).

The use of XRD allowed to identify the crystallographic orientation in terms of localization of crystals. Some organisms showed a similar crystalline phase, but lattice parameters *a*, *b* and *c* had different values (Pokroy et al., 2006); and preferential orientation presented considerable differences according to the evaluated section (Zhu et al., 2006). Lutts et al. (1960) identified the calcium carbonate phase for 19 mollusc species, using X-ray diffraction (Table 3). The authors verified that aragonite was not observed in several samples of prismatic material, which were rich in "conchiolin" fibrils. These results provide relevant information on the correlation among the crystalline phase, organic composition and morphological aspects.

Wilbur and Watabe (1963) have studied the regeneration process in a series of molluscan species. Some of them did not alter their crystalline phase during regeneration, whereas other species contain all the three polymorphs of calcium carbonate. The fossil species of cephalopods studied by Voss-Foucart and Grégoire (1971) present a correlation between the "conchiolin" matrix and the calcium carbonate polymorphs. In this case, aragonite is recrystallized into calcite.

The crystallographic structure of nacre layers from 50 molluscan species differ among bivalves, cephalopods, gastropods and monoplacophorans (Chateigner et al., 2000). This information shows that although molluscan shells are constituted of aragonite with similar microstructures, there is a difference in the preferential orientation according to the species. A fibrous texture occurred only in gastropods and cephalopods; double twin textures appeared only in bivalves and cephalopods. It should be noted that the correlation between microstructure and crystallographic orientation is not simple, and other features should be taken into account, such as biological composition, the molluscan shell layer and species.

Mapping of individual crystallite structure, performed by DiMasi and Sarikaya (2004), with synchrotron X-ray diffraction in the nacre-prismatic region of red abalone, confirmed the presence of millimeter-long calcite grains with preferential orientation in the (1 0 4) plane. Similar orientations were obtained by Runnegar (1984), who investigated the structure of foliated layers based on crystal faces of the calcite of some bivalves. On the other hand, results obtained for bivalves *Pecten albicans* and

Table 3
$CaCO_3$ crystallization types in some molluscan shells.

$CaCO_3$ polymorphs	Organisms
Calcite with traces of aragonite	1. *Turbo* sp. 2. Mytilus *edulis* L. 3. *Pinctada mazatlanica* Hanley
Calcite	4. *Vulsella vulsella* L. 5. *Malleus daemoniacus* Reeve 6. *Malleus regula* Forskal 7. *Pinctada margaritifera* L. 8. *Pinctada galtsoffi* Bartsch 9. *Ostrea edulis* L. 10. *Pinna nobilis* 11. *Atrina nigra* Durhenn 12. *Pteria pengin*
Aragonite	13. *Margaritana margaritifera* L. 14. *Unio rectus* Lamarck 15. *Anodonta cygnaea* L. 16. *Metaptera laevissima* Lea 17. *Metaptera fragilis* R.F.G. 18. *Anodontites trapezialis* Lamarck 19. *Iridina spekii* SP Woodward

From Lutts et al. (1960).

Amusium japonicum balloti showed strong peaks at the (1 0 8) orientation.

The process involving biogenic crystal formation is not fully understood yet. In fact, information on matrix–crystal correlation is essential to understand shell formation. The XRD provides information about the development of the crystalline structure, which is mediated by an organic matrix composed of proteins and glycoproteins.

Weiner and Traub (1980) have contributed with data on *Nautilus rupertus*. The nacreous layer has organic matrix (*a*, *b* and *c* axes) and an unoriented diffuse pattern, which was attributed to the prismatic layer. The X-ray pattern obtained for *Mytilus californianus* prismatic layer was characterized by a partial orientation, indicating that the protein β-pleated sheet had *a* and *b* axes randomly oriented in the plane of the specimen and *c* axis is perpendicular to this plane. Chitin was not observed in any of the following bivalves: *Crassostrea iridescens* (foliated layer), *P. radiata* (nacreous layer) and *M. californianus* (nacreous and prismatic layers). On the other hand, the X-ray patterns from the prismatic layer of *Tectus dentatus* were characteristic for chitin. The X-ray diffraction results have shown that the organic matter in individual layers has a different orientation. These characteristics may influence the crystallization process of calcium carbonate.

5.3.2. The Rietveld method

Some aspects involved in the molluscan shell formation, as quantification of the calcium carbonate crystalline phase, have not been extensively investigated. The Rietveld method is widely used as a tool for crystal structure analysis, quantitative phase analysis and, when needed, information about texture and material characteristics, like crystallite size and microstrain. This is a refinement method for a model of parameters involving crystal structure, instrumental and physical characteristics of the material. The objective is to refine this model to minimize the sum of the squared difference between the observed and calculated points of the diffractograms. Parameters of the unit cell, atom displacement (thermal parameters) and occupation factor can be adjusted using the Least-Square Method. When the refinement is completed, the results provide the quantitative phase analysis, precise cell parameters, preferred orientation information and chemical compositions. Considering that this is a parameter refinement method, an initial model is required and, subsequently, it is important to know the crystal structures of the crystalline phases (Young, 1995).

The Rietveld method has also contributed to information about calcium carbonate phase during shell development. Gómez-Martínez et al. (2002) have demonstrated that bivalve *Ischadium recurvum* contains aragonite internally and calcite externally. Both polymorphs are characterized by strong preferential orientation with high variation during shell growth. The X-ray diffraction results show evidence of the reliance on texture in the growth stage of this bivalve. Hasse et al. (2000) investigated the crystalline nature of *B. glabrata* shells: in the initial stage, the samples were completely amorphous, at 120 h age, they were constituted exclusively of pure aragonite, whereas in the oldest part of the shell (the center of the snail), little vaterite content was found, both phases were detected through Rietveld refinement. This method has proved to be an excellent tool to distinguish the different phases of calcium carbonate during the shell growth.

We used gastropods *A. fulica*, *P. cubensis* and bivalve *M. maculata* to investigate the mineral phase and analyze the orientation planes. Data were refined with the Rietveld method using GSAS software. According to our results, these shells are comprised of orthorhombic aragonite. Although the refinement shows the same polymorph for both samples, the diffraction peaks show different preferential orientation. The results for *A. fulica* shell present

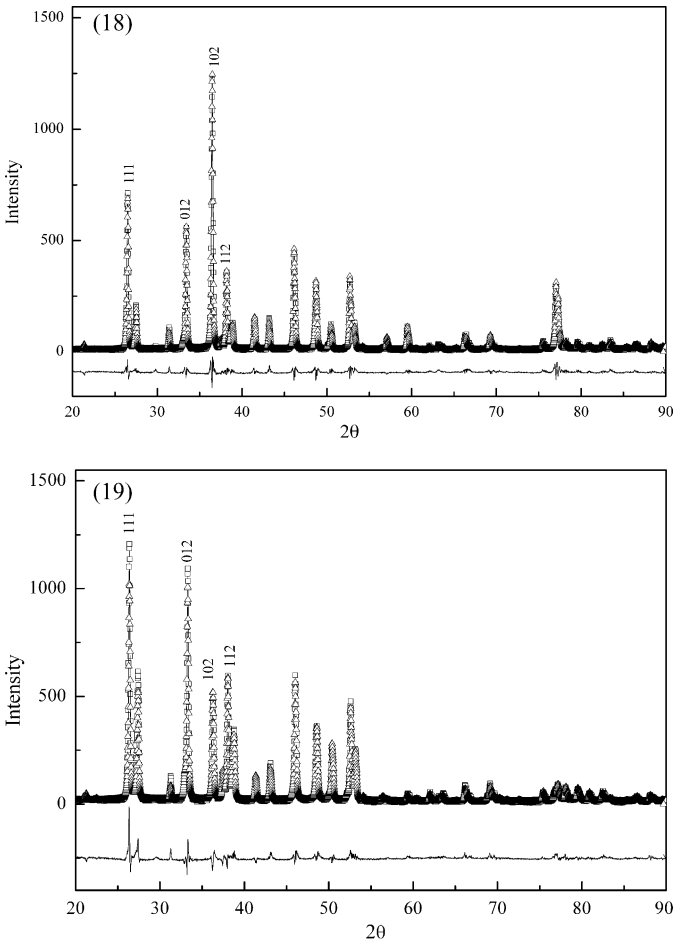

Figs. 18–19. Fitting result of Rietveld refinement demonstrating the typical spectrum of aragonite. Squares and triangles represent the observed and calculated profile intensities, respectively. The difference between calculated and observed intensities is given at the bottom of the diagram. The results show intense diffraction peaks in the (1 0 2) plane for *Achatina fulica* (Fig. 18); for *Macrocallista maculata* (Fig. 19). Intense peaks occur in (1 1 1) and (0 1 2) planes.

intense diffraction peaks in the (1 0 2) plane (Fig. 18), while for *M. maculata* this peak has low intensity (Fig. 19). Diffraction patterns from *P. cubensis* shells showed predominance of aragonite, although small amounts of calcite were present (0.6%) (De Paula and Silveira, 2005). Results obtained for this organism (Fig. 20) show diffraction peaks with similar orientation to those obtained for *M. maculata*. These results suggested that, although these molluscan shells are comprised of aragonite, lattice parameters *a*, *b* and *c* obtained differs from their geological aragonite and their crystalline arrangement has presented some morphological differences.

Comparing electron diffraction and X-ray diffraction, we can conclude that both provide important data about crystal structures and are complementary techniques. Both approaches present advantages and disadvantages: (a) the interaction of electrons with the sample is much stronger than with X-rays; consequently, the resolution in *d* spacing is better; (b) using electron diffraction in TEM it is possible to directly relate the diffractogram with the image of the sample. Samples must be of the order of 100 nm and should be electron transparent; only a single crystal or particle may be selected for analysis while X-ray diffraction provides overall information of the crystalline phase. When using the Rietveld method, for example, the results obtained from X-ray diffraction can be quantified, while electron diffraction is a qualitative technique; (c) time consuming and careful sample

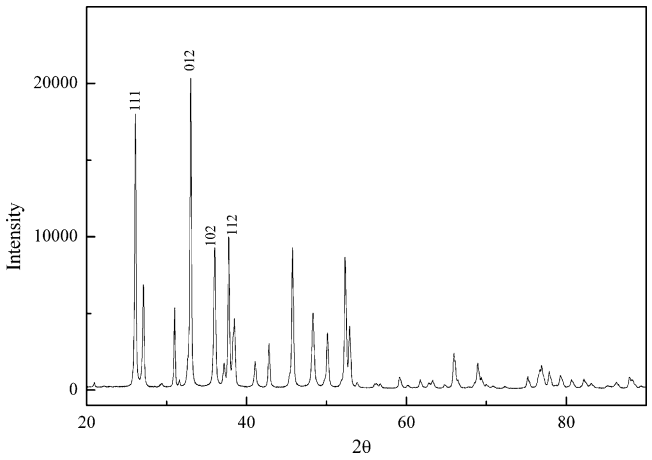

Fig. 20. X-ray diffraction pattern of powdered shell of adult *Physa cubensis* reveals that this molluscan shells mainly contain aragonite with intense peaks for (1 1 1) and (0 1 2) planes. There is no indication of a preferential orientation.

preparation may therefore be needed to prepare samples for the analysis by electron diffraction, while sample for X-ray diffraction experiments requires simple procedures. Despite these features, X-ray diffraction and electron diffraction are complementary techniques; their information can be added to understand crystal structures.

Acknowledgements

We feel indebted to the following specialists, for generous gifts of shells from their collections: Prof. Dr. Osmar Domaneschi (*in memoriam*) and Dr. Sonia Carvalho Lopes (Instituto de Biociências, USP); Dr. Toshie Kawano (Instituto Butantan); Ms Monica A. Varella Petti (Instituto Oceanográfico, USP). Prof. Domaneschi and Ms. Eliane P. de Arruda kindly ascertained identification of scaphopodan shells. Electron microscopes were grants from FINEP-PSME (#43.88.0525.00) and FAPESP (#93/4108-5). S.M. Paula was the recipient of a CNPq doctoral fellowship (#140929/2001-0). Prof. Dr. Henrique Toma, Drs. Isaac Sayeg, Anamaria Alexiou and Marcia A.C. Fantini, are thanked for access to their spectroscopic equipments, and Prof. Dr. Alberto A. Ribeiro and Márcio V. Cruz for access to the Zeiss DSM-940 TEM of the Instituto de Biociências, USP. Valuable assistance of Simone P. de Toledo, Rodrigo S. Tosi and Antonio C.F. da Silveira is greatly appreciated.

References

Abbott, R.T., 1974. American Seashells, 2nd ed. Van Nostrando Reinhold Co., New York, 663 pp.

Addadi, L., Weiner, S., 1992. Control and design principles in biological mineralization. Angew. Chem. Int. Ed. Engl., Wiley Interscience 31 (2), 153–169.

Addadi, L., Weiner, S., Geva, M., 2001. On how proteins interact with crystals and their effect on crystal formation. Z. Kardiol. 90 (Suppl. 3), III/92–III/98.

Addadi, L., Joester, D., Nudelman, F., Weiner, S., 2006. Mollusk shell formation: a source of new concepts for understanding biomineralization processes. Chem. Eur. J. 12, 980–987.

Albeck, S., Aizenberg, J., Addadi, L., Weiner, S., 1993. Interactions of various skeletal intracrystalline components with calcite crystals. J. Am. Chem. Soc. 115, 11691–11697.

Alzuria, M., 1985. Ultraestructura de la concha en *Dentalium vulgare* (Da Costa, 1778) (Mollusca: Scaphopoda). Iberus 5, 11–19.

Balmain, J., Hannover, B., Lopez, E., 1999. Fourier transform infrared spectroscopy (FTIR) and X-ray diffraction analysis of mineral and organic matrix during heating of mother of pearl (Nacre) from the shell of the mollusc *Pinctada maxima*. J. Biomed. Mater. Res. 48 (5), 749–754.

Bandel, K., 1990. Shell structure of the Gastropoda excluding Archaeogastropoda. In: Carter, J.G. (Ed.), Skeletal Biomineralization: Patterns, Processes and Evolutionary trends, vol. 1. Van Nostrand Reinhold, New York, pp. 117–134.

Berland, S., Delattre, O., Borzeix, S., Catonné, Y., Lopez, E., 2005. Nacre/bone interface changes in durable nacre endosseous implants in sheep. Biomaterials 26, 2767–2773.

Bevelander, G., Nakahara, H., 1967. An electron microscope study of the formation of the periostracum of *Macrocallista maculata*. Calcif. Tissue Res. 1, 55–67.

Bevelander, G., Nakahara, H., 1969. An electron microscope study of the formation of the ligament of *Mytilus edulis* and *Pinctada radiata*. Calcif. Tissue Res. 4, 101–112.

Bevelander, G., Nakahara, H., 1970. An electron microscope study of the formation and structure of the periostracum of a gastropod, *Littorina littorea*. Calcif. Tissue Res. 5, 1–12.

Bezares, J., Asaro, R.J., Hawley, M., 2008. Macromolecular structure of the organic framework of nacre in *Haliotis rufescens*: implications for growth and mechanical behavior. J. Struct. Biol. 163, 61–75.

Bøggild, O.B., 1930. The shell structure of the molluscs. Det Kongelige Danske Vidensk. Selskabs Skr. Naturv. og math. Afd., Ser. 9 II (2), 233–326.

Brugnerotto, J., Lizardi, J., Goycoolea, F.M., Argülles-Monal, W., Desbrières, J., 2001. An infrared investigation in relation with chitin and chitosan characterization. Polymer 42, 3569–3580.

Bubel, A., 1973a. An electron microscope study of periostracum formation in some marine Bivalves. I. The origin of the periostracum. Mar. Biol. 20, 213–221.

Bubel, A., 1973b. An electron microscope study of periostracum formation in some marine Bivalves. II. The cells lining the periostracal groove. Mar. Biol. 20, 222–234.

Callil, C.T., Mansur, M.C.D., 2005. Ultrastructural analysis of the shells of *Anodontites trapesialis* (Lamarck) and *Anodontites elongatus* (Swaison) (Mollusca, Bivalvia, Etherioidea) from the Mato Grosso Pantanal Region, Brazil. Rev. Bras. Zool. 22 (3), 724–734.

Carter, J.G., 1980a. Environmental and biological controls of bivalve shell mineralogy and microstructure. In: Rhoads, D.C., Lutz, R.A. (Eds.), Skeletal Growth of Aquatic Organisms. Biological Records of Environmental Change. Plenum Press, New York, London, (chapter 2), pp. 69–113.

Carter, J.G., 1980b. Guide to bivalve shell microstructures, Appendix 2, part B. In: Rhoads, D.C., Lutz, R.A. (Eds.), Skeletal Growth of Aquatic Organisms. Biological Records of Environmental Change. Plenum Press, New York, London, pp. 645–673.

Carter, J.G., 1990a. Shell microstructural data for the bivalvia. Ch.11, part I. Introduction. In: Carter, J.G. (Ed.), Skeletal Biomineralization: Patterns, Processes and Evolutionary Trends, vol. 1. Van Nostrand Reinhold, New York, pp. 297–301.

Carter, J.G., 1990b. Glossary of skeletal biomineralization (a compilation by Carter, J.G. et al.). In: Carter, J.G. (Ed.), Skeletal Biomineralization: Patterns, Processes and Evolutionary Trends, vol. 1. Van Nostrand Reinhold, New York, pp. 609–627.

Carter, J.G., Ambrose, W.W., 1989. Techniques for studying molluscan shell microstructure. In: Feldmann, R.M., Chapman, R.E., Hannibal, J.T. (Eds.), Paleotechniques. The Paleontological Society Special Publication Nr. 4.The University of Tennessee, Knoxsville, TN, (reprinted, 1997), pp. 101–119.

Cartwright, J.H.E., Checa, A.G., 2007. The dynamics of nacre self-assembly. J. R. Soc. Interface 4, 491–504.

Chateigner, D., Hedegaard, C., Wenk, H.R., 2000. Mollusc shell microstructures and crystallographic textures. J. Struct. Geol. 22, 1723–1735.

Checa, A.G., 2000. A new model for periostracum and shell formation in Unionidae (Bivalvia, Mollusca). Tissue Cell 32, 405–416.

Checa, A.G., Cadée, G.C., 1997. Hydraulic burrowing in the bivalve *Mya arenaria* Linnaeus (Myoidea) and associated ligamental adaptations. J. Mol. Stud. 63, 157–171.

Checa, A.G., Okamoto, T., Ramirez, J., 2006. Organization pattern of nacre in Pteriidae (Bivalvia: Mollusca) explained by crystal competition. Proc. R. Soc. B 273, 1329–1337.

Checa, A.G., Rodriguez-Navarro, A., 2001. Geometrical and crystallographic constraints determine the self-organization of shell microstructures in Unionidae (Bivalvia: Mollusca). Proc. R. Soc. Lond. B 268, 771–778.

Checa, A.G., Rodriguez-Navarro, A.B., 2005. Self-organisation of nacre in the shells of Pterioida (Bivalvia: Mollusca). Biomaterials 26, 1071–1079.

Checa, A., Rodriguez-Navarro, A.B., Esteban-Delgado, F.J., 2005. The nature and formation of calcitic columnar prismatic shell layers in pteriomorphian bivalves. Biomaterials 26, 6404–6414.

Compere Jr., E.L., Bates, J.M., 1973. Determination of calcite: aragonite ratios in mollusc shells by infrared spectra. Limnol. Oceanogr. 18 (2), 326–331.

Conley, R.T., 1966. Infrared Spectroscopy. Allyn and Bacon, Inc., Boston.

Cortie, M.B., McBean, K.E., Elcombe, M.M., 2006. Fracture mechanics of mollusc shells. Phys. B 385-386, 545–547.

Cruz, R., Weissmüller, G., Farina, M., 2003. Microstructure of Monoplacophora (Mollusca) shell examined by low-voltage field emission scanning electron and atomic force microscopy. Scanning 25, 12–18.

Currey, J.D., 1988. Shell form and strength. Chap. 8. In: Trueman, E.R., Clarke, M.R. (Eds.), The Mollusca, Vol. 11. Form and Function. Academic Press, Inc., pp. 183–210.

Currey, J.D., 1999. The design of mineralised hard tissues for their mechanical functions. J. Exp. Biol. 202, 3249–3285.

Dauphin, Y., 1999. Infrared spectra and elemental composition in recent biogenic calcites: relationships between the ν_4 band wavelength and Sr and Mg concentrations. Appl. Spectrom. 53 (2), 184–190.

Dauphin, Y., 2003. Soluble organic matrices of the calcitic prismatic shell layers of two Pteriomorphid bivalves. J. Biol. Chem. 278, 15168–15177.

Dauphin, Y., 2006. Structure and composition of the septal nacreous layer of *Nautilus macromphalus* L. (Mollusca, Cephalopoda). Zoology 109, 85–95.

Dauphin, Y., Ball, A.D., Cotte, M., Cuif, J.-P., Meibom, A., Salomé, M., Susini, J., Williams, C.T., 2008. Structure and composition of the nacre-prisms transition in the shell of *Pinctada margaritifera* (Mollusca, Bivalvia). Ann. Bioanal. Chem. 390, 1659–1669.

Dauphin, Y., Cuif, J.P., Doucet, J., Salomé, M., Susini, J., Williams, C.T., 2003a. In situ chemical speciation of sulfur in calcitic biominerals and the simple prism concept. J. Struct. Biol. 142, 272–280.

Dauphin, Y., Denis, A., 2000. Structure and composition of the aragonitic crossed lamellar layers in six species of Bivalvia and Gastropoda. Comp. Biochem. Physiol. A 126, 367–377.

Dauphin, Y., Guzman, N., Denis, A., Cuif, J.-P., Ortlieb, L., 2003b. Microstructure, nanostructure and composition of the shell of *Concholepas concholepas* (Gastropoda, Muricidae). Aquat. Living Resour. 16, 95–103.

De Paula, S.M., 2006. Uma abordagem de parâmetros da biomineralização em um sistema constituído por carbonato de cálcio. Doctoral Dissertation. Instituto de Física, Universidade de São Paulo, Brasil, 174 pp. (in Portuguese). http://www.teses.usp.br/teses/disponiveis/43/43134/tde-09022007-112553/.

De Paula, S.M., Silveira, M., 2005. Microstructural characterization of shell components in the mollusc *Physa* sp. Scanning 27, 120–125.

Delattre, O., Catonne, Y., Berland, S., Borzeix, S., Lopez, E., 1997. Use of mother of pearl as a bone substitute—experimental study in sheep. Eur. J. Orthop. Surg. Traumatol. 7, 143–147.

DiMasi, E., Sarikaya, M., 2004. Synchrotron X-ray microbeam diffraction from abalone shell. J. Mater. Res. 19, 1471–1476.

Dove, P.M., De Yoreo, J., Weiner, S. (Eds.), 2003. Reviews in Mineralogy and Geochemistry, vol. 54. Mineralogical Society of America, Washington.

Duplat, D., Chabadel, A., Gallet, M., Berland, S., Bédouet, L., Rousseau, M., Kamel, S., Milet, C., Jurdic, P., Brazier, M., Lopez, E., 2007. The in vitro osteoclastic degradation of nacre. Biomaterials 28, 2155–2162.

Emerson, W.K., 1962. A classification of the scaphopod mollusks. J. Paleontol. 36, 461–482.

Falini, G., Fermani, S., Ripamonti, A., 2002. Crystallization of calcium carbonate salts into beta-chitin scaffold. J. Inorg. Biochem. 91, 475–480.

Falini, G., Weiner, S., Addadi, L., 2003. Chitin–silk fibroin interactions: relevance to calcium carbonate formation in invertebrates. Calcif. Tissue Res. 72, 548–554.

Farre, B., Dauphin, Y., 2009. Lipids from the nacreous and prismatic layers of two Pteriomorpha Mollusc shells. Comp. Biochem. Physiol. B 152, 103–109.

Feng, Q.L., Cui, F.Z., Pu, G., Wang, R.Z., Li, H.D., 2000a. Crystal orientation, toughening mechanisms and a mimic of nacre. Mater. Sci. Eng. C11, 19–25.

Feng, Q.L., Li, H.B., Pu, G., Zhang, D.M., Cui, F.Z., Li, H.D., 2000b. Crystallographic alignment of calcite prisms in the oblique prismatic layer of *Mytilus edulis* shell. J. Mater. Sci. 35, 3337–3340.

Fischer-Piette, E., Franc, A., 1968. Classe des Scaphopodes. In: Grassé, P.-P. (Ed.), Traité de Zoologie. V. Fasc. III. Masson et Cie. Ed, Paris, pp. 987–1017.

Fratzl, P., Gupta, H.S., 2007. Nanoscale mechanisms of bone deformation and fracture. Chap. 23. In: Bäuerlein, E. (Ed.), Handbook of Biomineralization Biological and Structure Formation. Wiley–VCH Verlag GmbH & Co. KgaA, pp. 397–414.

Fritz, M., Belcher, A., Radmacher, M., Walters, D.A., Hansma, P.K., Stucky, G.D., Morse, D.E., Mann, S., 1994. Flat pearls from biofabrication of organized composites on inorganic substrates. Nature 371, 49–51.

Fu, G., Valiyaveettil, S., Wopenka, B., Morse, D.E., 2005. $CaCO_3$ biomineralization: acidic 8-kDa proteins isolated from aragonitic abalone shell nacre can specifically modify calcite crystal morphology. Biomacromolecules 6, 1289–1298.

Giles, R., Manne, S., Mann, S., Morse, D.E., Stucky, G.D., Hansma, P.K., 1995. Inorganic overgrowth of aragonite on molluscan nacre examined by atomic force microscopy. Biol. Bull. 188, 8–15.

Glauber, R., Schomaker, V., 1953. The theory of electron diffraction. Phys. Rev. 89 (4), 667–671.

Gómez-Martínez, O., Aguilar, D.H., Alvarado-Gil, J.J., Quintana, P., Aldana-Aranda, D., 2002. Texturization analysis by X -ray diffraction of shells of the mussel *Ischadium recurvum* (Rafinesque, 1820) (Mollusca Bivalvia). Mater. Res. Soc. 711, HH3.45.1–HH3.45.6.

Grégoire, Ch., 1960. Further studies on structure of the organic components in mother-of-pearl, especially in Pelecypods (Part I). Bull. Inst. R. Sci. Nat., Belgique 36 (23), 1–22.

Grégoire, Ch., 1961. Structure of the conchiolin cases of the prism in the *Mytilus Edulis Linne*. J. Biophys. Biochem. Cytol. 9 (2), 395–400.

Grégoire, Ch., 1967. Sur la structure des matrices organiques des coquilles de Mollusques. Biol. Rev. 42, 653–687.

Grégoire, Ch., 1972. Structure of the molluscan shell. Chap. 2. In: Florkin, M., Scheer, B.T. (Eds.), Chemical Zoology VII. Mollusca. Academic Press, New York, London, pp. 45–101.

Grégoire, Ch., 1974. On the organic and mineral components of the shells of Aetheriidae (Mollusca, Bivalvia, Unionacea). Rev. Zool. Afr. 88 (4), 847–896.

Haas, W., 1972. Micro and ultrastructure of recent and fossil Scaphopoda. In: 24th International Geological Congress. Montreal, Section 7, pp. 15–19.

Hasse, B., Ehrenberg, H., Marxen, J., Becker, W., Epple, 2000. Calcium carbonate modifications in the mineralized shell of the freshwater snail *Biomphalaria glabrata*. Chem. Eur. J. 20, 3679–3685.

Hickman, C.S., 2004. The problem of similarity: analysis of repeated patterns of microsculpture on gastropod larval shells. Invertebr. Biol. 123 (3), 198–211.

Hirsch, P.B., Nicholson, R.B., Howie, A., Pashley, D.W., Whelan, M.J., 1965. Electron Microscopy of Thin Crystals. Butterworths, London.

Hoshi, K., Ejiri, S., Ozawa, H., 2001. Organic components of crystal sheaths in bone. J. Electron Microsc. 50 (1), 33–40.

Hou, W.T., Feng, Q.L., 2003. Crystal orientation preference and formation mechanism of nacreous layer in mussel. J. Cryst. Growth 258, 402–408.

Jones, G.M., Saleuddin, S.M., 1978. Cellular mechanisms of periostracum formation in *Physa* spp. (Mollusca: Pulmonata). Can. J. Zool. 56 (11), 2299–2311.

Kähler, G.A., Sass, R.L., Fisher Jr., F.M., 1976. The fine structure and crystallography of the hinge ligament of *Spisula solidissima* (Mollusca: Bivalvia: Mactridae). J. Comp. Phys. 109, 209–220.

Kamat, S., Su, X., Ballarini, R., Heuer, A.H., 2000. Structural basis for the fracture toughness of the shell of the conch *Strombus gigas*. Nature 405, 1036–1040.

Kaplan, D.L., 1998. Mollusc shell structure: novel design strategies for synthetic materials. Curr. Opin. Sol. Mater. Sci. 3, 232–236.

Kim, Y.-W., Kim, J.-J., Kim, Y.H., Rho, J.-Y., 2002. Effects of organic matrix proteins on the interfacial structure at the bone-biocompatible nacre interface in vitro. Biomaterials 23, 2089–2096.

Kobayashi, I., Samata, T., 2006. Bivalve shell structure and organic matrix. Mater. Sci. Eng. C 26, 692–698.

Larson, A.C., Von Dreele, E.R.B., 2001. General Structure Analysis System (GSAS)-Los Alamos National Laboratory Report. Copyright 1985–2000. The Regents of the University of California.

Levi-Kalisman, Y., Falini, G., Addadi, L., Weiner, S., 2001. Structure of the nacreous organic matrix of a bivalve mollusk shell examined in the hydrated state using cryo-TEM. J. Struct. Biol. 135, 8–17.

Liao, H., Mutvei, H., Hammarström, L., Wurtz, T., Li, J., 2002. Tissue responses to nacreous implants in rat femur: an in situ hybridization and histochemical study. Biomaterials 23, 2693–2701.

Liao, H., Mutvei, H., Sjöström, M., Hammarström, L., Li, J., 2000. Tissue responses to natural aragonite (*Margaritifera* shell) implants in vivo. Biomaterials 21, 457–468.

Lin, A., Meyers, M.A., 2000. Growth and structures in abalone shell. Mater. Sci. Eng. 390, 27–41.

Lowenstam, H.A., Weiner, S., 1989. On Biomineralization. Oxford University Press, Inc., New York, Oxford, pp. 89–110.

Lutterotti, L., Matthies, S., Wenk, H.R., Schultz, A.J., Richardson, J.W., 1997. Combined texture and structure analysis of deformed limestone from time-of-flight neutron diffraction spectra. J. Appl. Phys. 81 (2), 594–600.

Lutts, A., Grandjean, J., Grégorie, Ch., 1960. X-Ray diffraction patterns from the prisms of mollusk. Arch. Int. Physiol. Biochim. 68, 829–831.

Mann, S., 1996. Biomineralization and Biomimetic Materials Chemistry. In: Mann, S. (Ed.), Biomimetical Materials Chemistry. Wiley–VCH, Weinheim, (chapter 1), pp. 1–40.

Mann, 1983. Mineralization in Biological Systems. Struct. Bonding 54, 125–174.

Mano, K., 1980. Scanning electron microscopy of the calcified ligament of some molluscs. In: Omori, M., Watabe, N. (Eds.), The Mechanisms of Biomineralization in Animals and Plants. Tokai University Press, Tokyo, pp. 99–106.

Marie, B., Luquet, G., Pais de Barros, J.-P., Guichard, N., Morel, S., Alcaraz, G., Bollache, L., Marin, F., 2007. The shell matrix of the freshwater mussel *Unio pictorum* (Paleoheterodonta, Unionoida). Involvement of acidic polysaccharides from glycoproteins in nacre mineralization. FEBS J. 274, 2933–2945.

Marin, F., Luquet, G., 2004. Molluscan shell proteins. Comptes Rendus Palevol 3, 469–492.

Marin, F., Luquet, G., 2005. Molluscan biomineralization: the proteinaceous shell constituents of *Pinna nobilis* L. Mater. Sci. Eng. C 25, 105–111.

Marin, F., Luquet, G., 2007. Unusually acidic proteins in biomineralization. In: Bäuerlein, E. (Ed.), Handbook of Biomineralization. Biological Aspects and Structure Formation. Wiley–VCH Verlag. GmbH & Co. KgaA, Weinheim, (chapter 16), pp. 271–290.

Marsh, M., Hopkins, G., Fisher, F., Sass, R.L., 1976. Structure of the molluscan bivalve hinge ligament, a unique calcified elastic tissue. J. Ultrastruct. Res. 54, 445–450.

Marsh, M.E., Sass, R.L., 1980. Aragonite twinning in the molluscan bivalve hinge ligament. Science 208, 1262–1263.

Marxen, J.C., Becker, W., 1997. The organic shell matrix of the freshwater snail *Biomphalaria glabrata*. Comp. Biochem. Physiol. 118 B, 23–33.

Marxen, J.C., Becker, W., Finke, D., Hasse, B., Epple, M., 2003. Early mineralization in *Biomphalaria glabrata*: microscopic and structural results. J. Mol. Stud. 69, 113–121.

Marxen, J.C., Hammer, M., Gehrke, T., Becker, W., 1998. Carbohydrates of the organic shell matrix and the shell-forming tissue of the snail *Biomphalaria glabrata* (Say). Biol. Bull. 194, 231–240.

Medakovié, D., 2000. Carbonic anhydrase activity and biomineralization process in embryos, larvae and adult blue mussels *Mytilus edulis* L. Helgoland Mar. Res. 54, 1–6.

Medakovié, D., Popovié, S., Grzeta, B., Plazonié, M., Hrs-Brenko, M., 1997. X-ray diffraction study of calcification processes in embryos and larvae of the brooding oyster *Ostrea edulis*. Mar. Biol. 129, 615–623.

Meenakshi, V.R., Hare, P.E., Watabe, N., Wilbur, K.M., 1969. The chemical composition of the periostracum of the molluscan shell. Comp. Biochem. Physiol. 29, 611–620.

Meenakshi, V.R., Martin, A.W., Wilbur, K.M., 1974. Shell repair in *Nautilus macromphalus*. Mar. Biol. 27, 27–35.

Meldrum, F.C., 2003. Calcium carbonate in biomineralisation and biomimetic chemistry. Int. Mater. Rev. 48 (3), 187–224.

Milet, C., Berland, S., Lamghari, M., Mouries, L., Jolly, C., Borzeix, S., Doumenc, D., Lopez, E., 2004. Conservation of signal molecules involved in biomineralisation control in calcifying matrices of bone and shell. Comptes Rendus Palevol 3, 493–501.

Mitchell, P.R., Phakey, P.P., 1995. Notes on the microstructure of the *Nautilus* shell. Scan. Microsc. 9, 215–230.
Nakahara, H., Bevelander, G., 1971. The formation and growth of the prismatic layer of *Pinctada radiata*. Calcif. Tissue Res. 7, 31–45.
Nassif, N., Pinna, N., Gehrke, N., Antonietti, M., Jäger, C., Cölfen, H., 2005. Amorphous layer around aragonite platelets in nacre. Proc. Natl. Acad. Sci. 102 (36), 12653–12655.
Nudelman, F., Gotliv, A.A., Addadi, L., Weiner, S., 2006. Mollusk shell formation: mapping the distribution of organic matrix components underlying a single aragonitic tablet in nacre. J. Struct. Biol. 153, 176–187.
Palmer, C.P., 1974. A supraspecific classification of the Scaphopod Mollusca. The Veliger 17 (2), 115–123.
Pereira-Mouriès, L., Almeida, M.J., Millet, C., Berland, S., Lopez, E., 2002a. Bioactivity of nacre water-soluble organic matrix from the bivalve mollusk *Pinctada maxima* in three mammalian cell types: fibroblast, bone marrow stromal cell and osteoblasts. Comp. Biochem. Physiol. B 132, 217–229.
Pereira-Mouriès, L., Almeida, M.J., Ribeiro, C., Peduzzi, J., Barthélemy, M., Millet, C., Lopez, E., 2002b. Soluble silk-like organic matrix in the nacreous layer of the bivalve *Pinctada maxima*. Eur. J. Biochem. 269, 4994–5003.
Pokroy, B., Fitch, A.N., Lee, P.L., Quintana, J.P., Caspi, E.N., Zolotoyabko, E., 2006. Anisotropic distortions in the mollusk-made aragonite: a widespread phenomenon. J. Struct. Biol. 152, 145–150.
Reynolds, P.D., 1997. The phylogeny and classification of Scaphopoda (Mollusca): an assessment of current resolution and cladistic reanalysis. Zool. Scr. 26 (1), 13–21.
Reynolds, P.D., 2002. The Scaphopoda. In: Southward, A.J., Tyler, P.A., Young, C.M., Fuiman, L.A. (Eds.), Advances in Marine Biology. Molluscan Radiation-Lesser Known Branches, 42. Academic Press/Elsevier MPG, Bodmin, UK, pp. 137–236.
Reynolds, P.D., Okusu, A., 1999. Phylogenetic relationships among families of the Scaphopoda (Mollusca). Zool. J. Linnean Soc. 126 (2), 131–154.
Rietveld, H.M., 1969. A profile refinement method for nuclear and magnetic structures. J. Crystallogr. 2, 65–71.
Rousseau, M., Lopez, E., Stempflé, P., Brendlé, M., Franke, L., Guette, A., Naslain, R., Bourrat, X., 2005. Multiscale structure of sheet nacre. Biomaterials 26, 6254–6262.
Runnegar, B., 1984. Crystallography of the foliated calcite shell layers of bivalve molluscs. Alcheringa 8, 273–290.
Ruthensteiner, B., Wanninger, A., Haszprunar, G., 2001. The protonephridial system of the tusk shell, *Antalis entalis* (Mollusca, Scaphopoda). Zoomorphology 121 (1), 19–26.
Saleuddin, A.S.M., 1971. Fine structure of normal and regenerated shell of *Helix*. Can. J. Zool. 49, 37–41.
Saleuddin, A.S.M., Hare, P.E., 1970. Amino acid composition of normal and regenerated shell of *Helix pomatia*. Can. J. Zool. 48, 886–888.
Saleuddin, A.S.M., Petit, H.P., 1983. The mode of formation and the structure of the periostracum. In: Saleuddin, A.S.M., Wilbur, K.M. (Eds.), The Mollusca Vol. 4, Part 1, Physiology. Academic Press Inc., London, pp. 199–234.
Salvini-Plawen, L.V., 1980. A reconsideration of systematics in the Mollusca (phylogeny and higher classification). Malacologia 19 (2), 249–278.
Schladitz, C., Vieira, E.P., Hermel, H., Möhwald, H., 1999. Amyloid-β-sheet formation at the air–water interface. Biophys. J. 77, 3305–3310.
Shimek, R.L., 1989. Shell morphometrics and systematics: a revision of the slender, shallow-water Cadulus of the Northeastern Pacific (Scaphopoda: Gadilida). The Veliger 32, 233–246.
Shimek, R.L., Steiner, G., 1997. Scaphopoda. In: Harrison, F.W., Kohn, A.J. (Eds.), Mollusca II: Microscopic Anatomy of Invertebrates, vol. 6B. Wiley–Liss, Inc., New York, pp. 719–781.
Sikes, C.S., Wheeler, A.P., Wierzbicki, A., Dillaman, R.M., De Luca, L., 1998. Oyster shell protein and atomic force microscopy of oyster shell folia. Biol. Bull. 194, 304–316.
Simkiss, K., Wilbur, K.M., 1989. Molluscs-epithelial control of matrix and minerals. In: Simkiss, K., Wilbur, K.M. (Eds.), Biomineralization: Cell Biology and Mineral Deposition Ch. 14. Academic Press, San Diego, pp. 230–260.
Simone, L.R.L., 2006. Land and Freshwater Molluscs of Brazil. EGB, Fapesp, São Paulo, 390 pp.
Song, F., Soh, A.K., Bai, Y.L., 2003. Structural and mechanical properties of the organic matrix layers of nacre. Biomaterials 24 (20), 3623–3631.
Su, X.-W., Zhang, D.-M., Heuer, A.H., 2004. Tissue regeneration in the shell of the giant queen conch, *Strombus gigas*. Chem. Mater. 16, 581–593.
Tan, T.L., Wong, D., Lee, P., 2004. Iridescence of a shell of mollusk *Haliotis glabra*. Opt. Express 12 (20), 4847–4854.
Taylor, J.D., Reid, D.G., 1990. Shell microstructure and mineralogy of the Littorinidae: ecological and evolutionary significance. Hydrobiologia 193, 199–215.
Toby, B.H., 2001. EXPGUI, a graphical user interface for GSAS. J. Appl. Cryst. 34, 210–221.
Tong, H., Hu, J., Ma, W., Zhong, G., Yao, S., Cao, N., 2002. In situ analysis of the organic framework in the prismatic layer of mollusk shell. Biomaterials 23, 2593–2598.
Toraya, H., 2000. Crystal structure refinement of α-Si_3N_4 using synchrotron radiation powder diffraction data: unbiased refinement strategy. Appl. Crystallogr. 33, 95–102.
Trueman, E.R., 1950. Observations on the ligament of *Mytilus edulis*. Q. J. Microsc. Sci. 91, 225–235.
Trueman, E.R., 1951. The structure, development, and operation of the hinge ligament of *Ostraea edulis*. Q. J. Microsc. Sci. 92, 129–140.
Veis, A., 2003. Mineralization in organic matrix frameworks. In: Dove, P.M., De Yoreo, J.J., Weiner, S. (Eds.), Biomineralization. Reviews in Mineralogy & Geochemistry, vol. 54Mineralogical Society of America/Geochemical Society, Blacksburg, pp. 249–289 (chapter 9).
Velázquez-Castillo, R.R., Reyes-Gasga, J., García-Gutierrez, D.I., Jose-Yacaman, M., 2006. Crystal structure characterization of *Nautilus* shell at different length scales. Biomaterials 27, 4508–4517.
Von Dreele, R.B., 1999. Combined Rietveld and stereochemical restraint refinement of a protein crystal structure. Calcif. Tissue Res. 32, 1084–1089.
Von Dreele, R.B., 2007. Multipattern Rietveld refinement of protein powder data: an approach to higher resolution. Calcif. Tissue Res. 40, 133–143.
Voss-Foucart, M.F., Grégoire, Ch., 1971. Biochemical composition and submicroscopic structure of matrices of nacreous conchiolinin fossil cephalopods (Nautiloids and Ammonoids). Bull. Inst. R. Sci. Natl. Belg. 47 (41), 1–41.
Wang, J., Xu, Y., Zhao, Y., Huang, Y., Wang, D., Jiang, L., Wu, J., Xu, D., 2003. Morphology and crystalline characterization of abalone shell and mimetic mineralization. J. Cryst. Growth 252, 367–371.
Warren, B.E., 1969. X-ray diffraction. Addison-Wesley Publishing Company, London (chapters 5, 6 and 7).
Watabe, N., 1956. Dahllite identified as a constituent of prodissoconch I, of *Pinctada martensii* (Dunker). Science 5, 630.
Watabe, N., 1965. Studies on shell formation XI: crystal–matrix relationships in the inner layers of mollusks shells. J. Ultrastruct. Res. 12, 351–370.
Watabe, N., 1981. Crystal growth of calcium carbonate in the Invertebrates. Prog. Cryst. Growth Charact. 4, 99–147.
Watabe, N., 1983. Shell repair. In: Saleuddin, A.S.M., Wilbur, K.M. (Eds.), The Mollusca. 4, Part 1, Physiology. Academic Press Inc., New York, pp. 289–316.
Watabe, N., 1984. Shell. In: Bereiter-Hahn, J., Matoltsy, A.G., Richards, S. (Eds.), Biology of the Integument, 1. Invertebrates. Springer-Verlag, Berlin, Heidelberg, New York, Tokyo, pp. 448–485.
Watabe, N., 1988. Shell structure. In: Trueman, E.R., Clarke, M.R. (Eds.), The Mollusca, 11. Form and Function. Academic Press, Inc., San Diego, (chapter 4), pp. 69–104.
Weiner, S., Addadi, L., 1997. Design strategies in mineralized biological materials. J. Mater. Chem. 7 (5), 689–702.
Weiner, S., Dove, P.M., 2003. An overview of biomineralization processes and the problem of the vital effect. In: Dove, P.M., De Yoreo, J.J., Weiner, S. (Eds.), Biomineralization, 54. Reviews in Mineralogy and Geochemistry. Mineralogical Society of America/Geochemical Society, pp. 1–29.
Weiner, S., Hood, L., 1975. Soluble protein of the organic matrix of mollusk shells: a potential template for shell formation. Science 190, 987–989.
Weiner, S., Traub, W., 1980. X-ray diffraction study of the insoluble organic matrix of mollusk shells. FEBS Lett. 111 (2), 311–316.
Weiner, S., Traub, W., Wagner, H.D., 1999. Lamellar bone: structure–function relations. J. Struct. Biol. 128, 241–255.
Weiner, S., Wagner, H.D., 1998. The material bone: structure–mechanical function relations. Ann. Rev. Mater. Sci. 28, 271–298.
Weiss, I.M., Renner, C., Steigl, M.G., Fritz, M., 2002a. A simple and reliable method for the determination and localization of chitin in Abalone nacre. Chem. Mater. 14, 3254–3259.
Weiss, I.M., Tuross, N., Addadi, L., Weiner, S., 2002b. Mollusc larval shell formation: amorphous calcium carbonate is a precursor phase for aragonite. J. Exp. Zool. 293, 478–491.
Weiss, I.M., Schönitzer, V., 2006. The distribution of chitin in larval shells of the bivalve mollusk *Mytilus galloprovincialis*. J. Struct. Biol. 153, 264–277.
Westbroek, P., Marin, F., 1998. A marriage of bone and nacre. Nature 392, 861–862.
Wilbur, K.M., 1964. Shell formation and regeneration. In: Wilbur, K.M., Yonge, C.M. (Eds.), Physiology of Mollusca. Academic Press, New York and London, pp. 243–282.
Wilbur, K.M., 1972. Shell formation in mollusks. In: Florkin, M., Scheer, B.T. (Eds.), Chemical Zoology VII. Academic Press, New York, London, pp. 103–145.
Wilbur, K.M., Saleuddin, A.S.M., 1983. Shell formation. In: Saleuddin, A.S.M., Wilbur, K.M. (Eds.), The Mollusca Vol. 4, Part 1, Physiology. Academic Press Inc., London, pp. 235–287.
Wilbur, K.M., Watabe, N., 1963. Experimental studies on calcification in molluscs and the alga *Coccolithus huxleyi*. Ann. N. Y. Acad. Sci. 109, 82–112.
Winick, H., Doniach, S., 1980. Synchrotron Radiation Research. Plenum Press, New York.
Wise Jr., S.W., 1970. Microarchitecture and mode of formation of nacre (mother-of-pearl) in Pelecypods, Gastropods, and Cephalopods. Eclogae Geol. Helv. 63 (3), 775–797.
Young, R.A., 1995. The Rietveld Method. International Union of Crystallography. Oxford University Press, Oxford.
Zhang, C., Zhang, R., 2006. Matrix proteins in the outer shell of Molluscs. Mar. Biotechnol. 8, 572–586.
Zhang, G.-S., 2007. Photonic crystal type structure in bivalve ligament of *Pinctada maxima*. Chin. Sci. Bull. 52 (8), 1136–1138.
Zhu, Z., Tong, H., Ren, Y., Hu, J., 2006. *Meretrix lusoria*—a natural biocomposite material: in situ analysis of hierarchical fabrication and micro-hardness. Micron 37, 35–40.